Journal of Energy Storage 33 (2021) 101724

Contents lists available at ScienceDirect

Journal of Energy Storage

journal homepage: www.elsevier.com/locate/est

Evaluation of the efficiency and resulting electrical and economic losses of photovoltaic home storage systems

Nina Munzke*, Bernhard Schwarz, Felix Büchle, Marc Hiller

Karlsruhe Institute of Technology (KIT), Hermann-von-Helmholtz-Platz 1, 76344 Eggenstein-Leopoldshafen

ARTICLE INFO

Keywords:
PV home storage systems
Efficiency evaluation
Performance
Economic evaluation

ABSTRACT

The increase in electricity prices along with a decrease in the price of storage systems has led to a rapid expansion of the photovoltaic (PV) home storage system market, particularly in Germany. In order to be economically viable, PV home storage systems must fulfil certain performance criteria. The overall performance and achievable self-sufficiency ratio of a PV battery home storage system depends on (i) the efficiencies of the system components, (ii) the standby consumption, (iii) the reaction time of the home storage system as well as (iv) the intelligence of the overall system control software. So far, PV home storage system still show very big differences in their performance. However, poor system performance can result in the system being no longer economic viable. Up to now, there have been only a few studies that deal with the evaluation and systematic comparison of the performance of PV home storage systems. For this paper the performance of 12 commercially available PV-battery systems has been analysed with a focus on the overall system efficiency. The efficiency of the systems is mainly influenced by the battery efficiency, power conversion efficiency and standby consumption of the different system components. Therefore, a testing and evaluation method has been developed. In this work the method as well as the results of the systems are presented. A detailed study of the influence of the effects of the individual losses on both total energy and monetary losses was carried out. It is shown that power conversion has the greatest influence on energy and monetary losses. For the systems under evaluation the monetary losses per year due to battery efficiency losses range between 2 €/a and 40 €/a. Monetary losses due to conversion losses range between 33 €/a and 137 €/a and due to standby consumption between 1 €/a and 46 €/a. The individual losses can be summed up to give a total loss, which lies between 44 €/a and 174 €/a.

1. Introduction

Energy storage systems, in particular those employing lithium-ion batteries, coupled with renewable energy sources are set to play a vital role in ensuring a reliable and clean energy supply, and are thus an important part of the energy transition. A significant increase in the market penetration of such systems depends to a large degree on their cost effectiveness within the specific application. Recent price reductions [1,2] as well as rapid technological developments in the home storage system market have resulted in several systems on the German market that are already economically favourable as compared to simple grid-connected electricity consumption [3,4]. In this context it is important to note that it is not only the up-front purchasing costs but also the quality and performance of a storage system that have a significant influence on the total cost. System performance is influenced by the efficiency of the different PV home storage system components as well as by the control quality and control strategy [5–9]. However, in the following the term system performance mainly refers to the system efficiency and the control quality. Individual studies have already dealt with the performance analysis of storage systems. Benatiallah et al. and Ma et al., for example, evaluate the performance of a PV home storage system in real use by analysing the losses of individual components [10,11]. Yet in order to be able to compare systems with each other before installation, methods are necessary to evaluate the performance not only in the installed state. First suggestions for the characterization of storage system performance can be found in Braun et al. [12]. However, the publication does not include measurement data. In March 2017 the first version of the “Efficiency Guideline for PV-storage systems” [13] was published. Since July 2019 a second version is available [14]. The document describes measurement procedures to determine the efficiency of the battery, the efficiency of the power conversion paths, the standby consumption and the control quality of PV home storage systems. The measurement procedures are performed on PV home storage systems that are integrated within a hardware-in-the-loop

* Corrending author.
E-mail address: nina.munzke@kit.edu (N. Munzke).

https://doi.org/10.1016/j.est.2020.101724
Received 15 April 2020; Received in revised form 17 July 2020; Accepted 3 August 2020

Nomenclature

f	filtered
X	placeholder for the different losses
d	day
y	year
$E_{L,X,y}$	energy losses X during one year /kWh
$E_{L,X,d}$	energy losses X during one day /kWh
e	reduction in grid feed-in
gc	increase in grid consumption
$E_{L,X,e}$	energy losses X that lead to a reduction in grid feed-in /kWh
$E_{L,X,gc}$	energy losses X that lead to an increase in grid consumption /kWh
$E_{L,PV2AC}$	energy losses of path PV2AC /kWh
$E_{L,PV2BAT\&AC,grid}$	energy losses of path PV2BAT&AC when grid feed in takes place/kWh
$E_{L,PV2BAT\&AC,HH}$	energy losses of path PV2BAT&AC when no grid feed in takes place/kWh
$E_{L,PV2BAT\&AC}$	energy losses of path PV2BAT&AC /kWh
$E_{L,AC2BAT}$	energy losses of path AC2BAT /kWh
$E_{L,PV\&BAT2AC}$	energy losses of path PV&BAT2AC /kWh
$E_{L,BAT2AC}$	energy losses of path BAT2AC /kWh
$E_{sby,DC,PV}$	standby consumption on the DC side of the PV inverter/PV input of the DC side of the inverter /kWh
$E_{sby,DC,BAT}$	standby consumption on the DC side of the battery inverter/ battery input of the DC side of the inverter (DC-coupled system) /kWh
$E_{sby,AC,PV}$	standby consumption on the AC side of the PV inverter (AC-coupled system) /kWh
$E_{sby,AC,BAT}$	standby consumption on the AC side of the battery inverter (AC-coupled system) /kWh
$E_{sby,AC,INV}$	standby consumption on the AC side of the inverter (DC-coupled system) /kWh
E_{periph}	energy consumption of all peripherical components /kWh
$E_{L,MPPT}$	MPP tracking losses /kWh
$E_{L,MPPT,grid}$	MPP tracking losses when grid feed in takes place /kWh
$E_{L,MPPT,HH}$	MPP tracking losses when no grid feed in takes place /kWh
Eff_{BAT}	battery efficiency /%
Eff_{SYS}	system efficiency /%
$E_{DC,BAT,dischg}$	energy discharged from the battery /kWh
$E_{DC,BAT,chg}$	energy charged in the battery /kWh
$E_{L,BAT}$	losses of the battery /kWh
$E_{L,BAT,dischg}$	losses of the battery during battery discharging /kWh
$E_{L,BAT,chg}$	losses of the battery during battery charging /kWh
E_{SC}	energy directly consumed by the system operator /kWh
E_{FI}	energy fed onto the grid /kWh
$E_{DC,PV}$	energy yield of the PV plant /kWh
$n_{ref.d}$	number of reference days per type of day of the VDI 4655 classification
all ref.d	all reference days
T	true
F	false
$P_{AC,PV,l}$	PV power with is not used to charge the battery /kW
$P_{sby,AC,BAT}$	AC standby power of the battery inverter /kW
$P_{AC,sby,PV}$	AC standby power of the PV inverter /kW
$P_{DC,PV}$	DC PV power /kW
$P_{AC,PV}$	AC PV power (AC-coupled system) /kW
$P_{DC,BAT}$	DC battery power /kW
$P_{AC,BAT}$	AC battery power (AC-coupled system) /kW
$P_{AC,INV}$	power on the AC side of the inverter (DC-coupled system) /kW
P_{SYS}	power of the whole PV home storage system /kW
P_{LOAD}	load of the HH /kW
P_{GRID}	power measured at the grid connection point /kW
$P_{DC,PV,t}$	DC PV target power /kW
$P_{AC,CONS}$	total AC power /kW
$P_{AC,CONS,PV}$	total AC power supplied by PV /kW
$P_{AC,CONS,l}$	AC power not covered by battery discharging /kW
$P_{GRID,PV}$	excess PV power /kW
P_{periph}	power consumption of all peripherical components /kW
$fact_{gc,X}$	grid consumption factor
$fact_{gc,BAT,chg}$	grid consumption factor battery charging
$fact_{gc,BAT,dischg}$	grid consumption factor battery discharging
$fact_{gc,BAT2AC}$	grid consumption factor of the path BAT2AC
$fact_{gc,PV\&BAT2AC}$	grid consumption factor of the path PV&BAT2AC
$fact_{gc,PV2BAT\&AC,HH}$	grid consumption factor of the path PV2BAT&AC when no grid feed in takes place
$fact_{gc,AC2BAT}$	grid consumption factor of the path AC2BAT
$fact_{gc,sby,DC,BAT}$	grid consumption factor standby consumption on the DC side of the battery inverter/ battery input of the DC side of the inverter (DC-coupled system)
$fact_{gc,MPPT,HH}$	grid consumption factor of MPPT losses when no grid feed in takes place
$U_{cell,chg,max}$	maximum cell voltage that occurs during the day being evaluated /V
$U_{cell,max,t}$	maximum cell voltage that has occurred during the complete reference day measurements /V
$U_{th,max}$	voltage offset for calculating a voltage threshold value above which the battery is considered fully charged /V
$U_{cell,chg,t2}$	cell voltage values lower than $U_{cell,max,t}$ - $U_{th,max}$ /V
$U_{cell,dischg,min}$	minimum cell voltage that occurs during the day being evaluated /V
$U_{cell,min,t}$	minimum cell voltage that has occurred during the complete reference day measurements /V
$U_{th,min}$	voltage offset for calculating a voltage threshold value below which the battery is considered completly discharged
$U_{cell,dischg,t2}$	cell voltage values higher than $U_{cell,min,t}$ - $U_{th,min}$ /V
$U_{cell,t1}$	cell voltage at the time t_1 /V
t_1	time during the measument
n_1	length of the data vector (measurement) being evaluated
$t_{UCell,dischg,min}$	vector with the time when the battery is empty
$t_{UCell,ch,max}$	vector with the time when the battery is full
$t_{full,empty}$	vector with the time when the battery is full or empty
$Seq_{full,empty}$	sequence with fully charged and discharged states during the day {0,1}
t_3	timestep of the vectors $t_{full,empty}$ and $Seq_{full,empty}$
n_2	length of the vector $Seq_{full,empty}$
$P_{L,X}$	power losses X that lead /kW

test environment. The power as well as the voltage and current are measured at various points by sensors integrated within the test environment. Results of various storage systems tested in the lab according to the efficiency guideline have already been published by Messner et al. and Munzke et alii. The published results show large differences between the individual systems [8,15]. These measurements are very useful for comparing different system characteristics, but they cannot be used to determine efficiency and performance in real applications. In addition, Kairies et al. and Figgener et al. used the definitions of the guideline and thus evaluated field measurement data [16,17]. However, since the load data and environmental conditions differ between the individual systems, this approach leads to less comparable results. Therefore, different approaches have been developed to evaluate the actual efficiency of the storage systems in the application and at the same time to ensure the highest possible comparability. One solution proposed is a simulation-based approach [9,18,19]. As input parameters, data sheet data determined on the basis of the efficiency guideline [13,14] are used. An ideal storage system without losses is compared with the real system. The simulation can be used to derive loss-induced increases in grid consumption and loss-induced decreases in grid feed-in and thus calculate a performance index. A comparison of different storage systems using the above described method was published by Weniger et al. [20–22]. In a second approach, a reference profile of different typical days is measured in the lab. Both a reference load and a reference PV profile are defined. These profiles consist of a sequence of different typical days which occur within one year. Niedermeyer et al. [23] uses the measurement results to calculate three performance indicators. They comprise the energy conversion, the control quality and the achievable self-sufficiency. Depending on the result achieved, the storage systems are classified into categories A to E for each criterion. In comparison, Orth et al. [24] compare the measurement results of a reference week with the simulation results of the corresponding ideal storage system and calculates a performance index based on loss-induced increases in grid consumption and loss-induced decreases in grid feed-in. In this paper, a more detailed approach is used, which applies reference profiles of individual days as described in [25]. The systems are compared on the basis of the system efficiency described in [8]. In order to show in detail where the greatest differences between the systems come from and where the greatest losses occur, the measurement results are analysed and compared with measssssurements according to the efficiency guideline. For this, however, simulation of the storage behaviour as described in other work [9,18,19] is not necessary. Finally, losses are compared from an energetic and an economic point of view. Individual studies have already considered the efficiency of storage systems more or less precisely, in simulation and for the dimensioning of storage systems. However, these do not serve the direct comparison of individual systems and system characteristics, but to illustrate the economic efficiency of storage systems as a function of different boundary conditions [26,27]. The present work shows a large overview of different systems, which were all operated in the same way in the laboratory. Thus the described methodology is validated on the basis of a large data base.

Table 1 shows an overview over the literature available in the context of performance evaluation of PV home storage systems.

2. Method

2.1. Storage systems under test

The different test procedures were applied to 20 storage systems and the results analysed. 4 out of the 20 systems have either been taken out of operation for safety or EMC reasons or have already failed are defective and were partly replaced. In order to present the results as clearly as possible, 12 systems with data sets that are as complete as possible were selected (see Table 2). The systems were bought between early 2016 and mid-2017 and are all systems with a Li-Ion battery.

The usable battery capacity is defined as the capacity that is available to the system operator during normal operation. These values were determined using cycle tests according to [13] and represent the average of all cycles, i.e. the average value of the energy with which the battery was discharged.

Table 2 also shows the rated output power of the power electronic components. These were also determined according to the efficiency guidelines [13].

Table 1
Literature overview.

	Field measurements /real use	Lab measurements		Determination of individual losses using real profiles		Comparison of the losses		Validation of results
Covered in the work	Investigation of the losses of individual components in field measurement data	Methodology for determining the efficiency of the individual components	Methodology for determining the efficiency of the system in operation	simulation based	based on measurement data	/ kWh	/ €	Validation of results by comparing real systems
Covered	[16,17]	[13–15]		[9,18,20–22]		[9,18,20–22,24]		[9,18,20–22]
Partially covered	[10,11]		[23,24]	[24]			[9,18,20–22,24]	[15,24]
Slightly covered			[12]	[23]	[10,11,23]	[10,11]		[10,11]
Current paper			x		x	x	x	x

Table 2
Overview of capacity and rated output power of storage systems under test.

System	A	B	C	D	E	F	G	H	I	J	K	L
Topology	AC	AC	AC	DC	DC	DC	AC	DC	DC	DC	DC	DC
Usable battery capacity /kWh	4.0	3.7	2.3	4.4	2.0	4.6	3.9	3.8	4.6	3.0	3.8	4.3
$P_{BESS,nom}$ (discharging) /$P_{AC,nom\ (discharging)}$ /kW	1.9	2.5	0.8	1.3	1.7	1.8	2.1	3.7	3.1	2.3	2.2	1.3
$P_{BAT,nom}$ (charging) /kW	1.1	2.6	0.8	1.4	1.8	2.0	2.3	2.5	3.5	2.6	2.6	1.3
$P_{PV\text{-}INV,nom}$ / $P_{AC,nom}$ (export) /kW	2.9	3.6	3.6	3.5	3.6	4.3	3.6	4.7	4.6	3.0	5.8	3.6

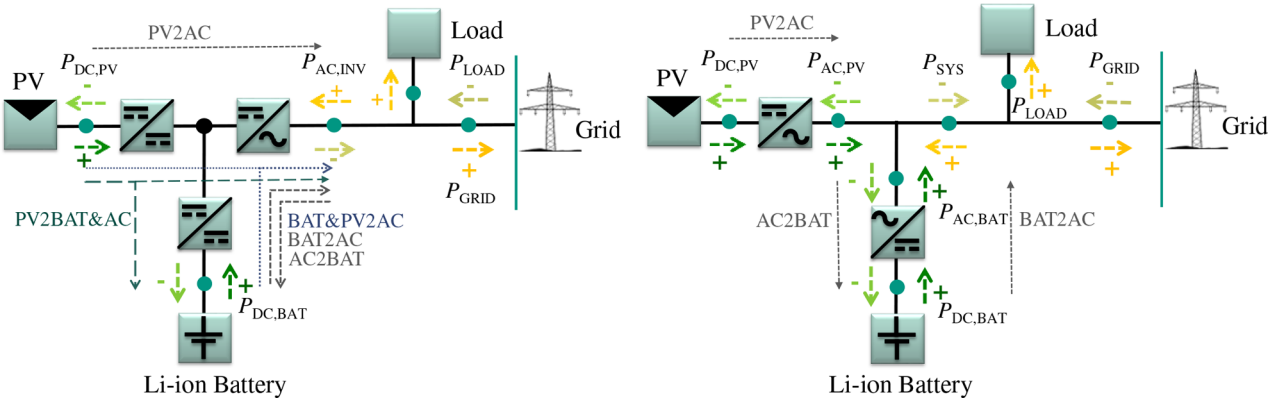

Fig. 1. Schematic of an AC-coupled (left) and a DC-coupled (right) PV home storage system including possible power flows and the corresponding symbols.

2.2. Measurement apparatus and system overview

The home storage systems are tested within a Power hardware-in-the-loop test environment, as detailed specified in the Efficiency Guidelines for PV-storage Systems [13]. Load and PV generators are used to emulate the households and PV system, respectively, and both are controlled by a LabVIEW program, with a communication rate of 200 ms, for both data recording and setting new target values. The home storage systems themselves decide whether to charge or discharge the battery, depending on the direction of the power flows with respect to the grid. The power as well as voltage and current are measured by sensors integrated within the test environment. A schematic of an AC-coupled and a DC-coupled PV home storage system including possible power flows can be found in Fig. 1. The variables are used in the Eqs. (11) to (61).

2.3. Input data and test procedure

Reference day measurements require typical load and generation profiles as a data basis. For the tests described in this work, real PV data with a sampling rate of 1 Hz from the 1 MW solar-storage park at KIT's north campus were used. The data were recorded from an array with southerly orientation (0°) and an inclination angle of 30°, which corresponds to a typical house with south-facing pitched roof. The PV system size was chosen to be 3.5 kWp. In order to generate appropriate and reproducible load profile data for a single family household (HH) the VDI 4655 standard [28] was used. It describes 10 different types of reference days during the year that make up the synthetic year. The reference household upon which the results in this work are based has an annual electricity consumption of 4200 kWh and corresponds to a five-person household in the VDI 4655 classification. The load profile stems from region 12 of the VDI 4655 profiles, which matches the location where the PV data was sourced (Karlsruhe), and the data has a sampling time of one minute. To validate the results, measured load data from the "ADRES-CONCEPT" research project [29] at TU Wien were employed. In this project the load data of 30 different Austrian single-family households were recorded at 1 Hz for one winter and one summer week. The households 06, 14, 16, 17, 19, 20, 23, 25 und 29, with an extrapolated annual consumption of between 2979 - 5399 kWh (see Table 3), were chosen for this study. To ensure that the batteries' initial state of charge (SOC) at the beginning of the day correspond with the final SOC at the end of the day, three identical reference days were measured in a row where the first day of measurements served as a form of calibration of the SOC (test 1). In the case of test 2, the last day of the week was used as the calibration day and then the whole week was measured. Furthermore, the measurements were started shortly before sunrise with an empty battery. Subsequently, only the days on which the battery voltage difference between the start and end of the measurement was almost identical were included in the evaluation of the data. As mentioned, additional measurements according to the Efficiency Guidelines version 2 were carried out.

2.4. Evaluation of the measurements

The reference day measurement procedure allows one to calculate the following quantities for each household:

- Average efficiency of both the battery (Eff_{BAT}) as well as the PV home storage system as a whole (Eff_{SYS}) (Eqs. (1) to (4)).
- Losses per year in kWh as well as in € due to conversion losses, standby consumption and battery efficiency

For test 1 these quantities can be calculated for a synthetic year using Eqs. (1), (3) and (5) to (61) below. The parameter $n_{ref,d}$ represents the number of reference days per type of day for region 12 (Karlsruhe) of the VDI 4655 classification. Ten different type days are described, four winter days, four transition days and two summer days. Four out of the ten days are holidays. In addition they vary between clear and cloudy days. In the following the subscript "d" stands for the evaluation of one reference day.

2.4.1. System and battery efficiency

$E_{DC,BAT,dischg,d}$ describes the energy discharged during one reference

Table 3
Test criteria for the reference day measurements.

	Test 1	Test 2
Load data	VDI 4655 - TRY 12 [28]	Household 06, 14, 16, 17, 19, 20, 23, 25 und 29 from the "ADRES-CONCEPT" project [29]
Annual electricity consumption/ persons per household	4200 kWh / 5 persons	~ 2979 - 5399 kWh
PV data	5 different days corresponding to the load reference days	7 summer & 7 winter days
PV system size	3.5 kWp	3.5 kWp

Table 4
Overview of the losses that occur and their categorisation as losses that lead to an increased grid consumption or a reduced grid feed-in.

	AC-System		DC-System	
	Increase of grid consumption	Decrease of grid feed in	Increase of grid consumption	Decrease of grid feed in
Battery efficiency	$E_{L,BAT,chg,gc}$ $E_{L,BAT,dischg,gc}$	$E_{L,BAT,chg,e}$ $E_{L,BAT,dischg,e}$	$E_{L,BAT,chg,gc}$ $E_{L,BAT,dischg,gc}$	$E_{L,BAT,chg,e}$ $E_{L,BAT,dischg,e}$
Power conversion	$E_{L,PV2AC,gc}$ - $E_{L,AC2BAT,gc}$ - $E_{L,BAT2AC,gc}$	$E_{L,PV2AC,e}$ - $E_{L,AC2BAT,e}$ - $E_{L,BAT2AC,e}$	$E_{L,PV2AC,gc}$ $E_{L,PV2BAT\&AC,gc}$ $E_{L,AC2BAT}$ $E_{L,PV\&BAT2AC,gc}$ $E_{L,BAT2AC,gc}$	$E_{L,PV2AC,e}$ $E_{L,PV2BAT\&AC,e}$ - $E_{L,PV\&BAT2AC,e}$ $E_{L,BAT2AC,e}$
Standby	$E_{sby,DC,PV}$ $E_{sby,DC,BAT,gc}$ $E_{sby,AC,PV}$ $E_{sby,AC,BAT,gc}$ $E_{periph,gc}$	- $E_{sby,DC,BAT,e}$ - $E_{sby,AC,BAT,e}$ $E_{periph,e}$	$E_{sby,DC,PV}$ $E_{sby,DC,BAT,gc}$ $E_{sby,AC,INV}$ $E_{periph,gc}$	- $E_{sby,DC,BAT,e}$ - $E_{periph,e}$
MPP tracking	$E_{L,MPPT,gc}$	$E_{L,MPPT,e}$	$E_{L,MPPT,gc}$	$E_{L,MPPT,e}$

day (measured on the DC side) and $E_{DC,BAT,chg,d}$ the energy stored within the battery. $E_{SC,d}$ is the energy directly consumed by the system operator per day, $E_{FI,d}$ the energy fed into the grid per day and $E_{DC,PV,d}$ the energy yield of the PV plant per day. For test 2 the results were simply summed up over each respective week (see. Eqs. (2) and (4)).

$$Eff_{BAT} = \frac{\sum_{\text{all ref.d}} (E_{DC,BAT,dischg,d} \cdot n_{ref.d})}{\sum_{\text{all ref.d}} (E_{DC,BAT,chg,d} \cdot n_{ref.d})} \cdot 100\ \% \quad (1)$$

$$Eff_{BAT} = \frac{E_{DC,BAT,dischg}}{E_{DC,BAT,chg}} \cdot 100\ \% \quad (2)$$

$$Eff_{SYS} = \frac{\sum_{\text{all ref.d}} ((E_{SC,d} + E_{FI,d}) \cdot n_{ref.d})}{\sum_{\text{all ref.d}} (E_{DC,PV,d} \cdot n_{ref.d})} \cdot 100\ \% \quad (3)$$

$$Eff_{SYS} = \frac{(E_{SC} + E_{FI})}{E_{DC,PV}} \cdot 100\ \%, \quad (4)$$

2.4.2. Overview of the different losses during operation

Losses (E_L) during operation include, among others, conversion losses, battery efficiency losses ($E_{L,BAT}$), MPP tracking losses and standby consumption. The higher the losses are, the lower the system efficiency. Table 4 gives an overview of the different losses for AC- as well as for DC-coupled systems. While losses that occur during charging are marked with "chg", losses that occur during discharging are marked with "dischg". The additional labelling of the losses with AC and DC indicates whether the losses occur on the DC or AC side of a component. Losses can either lead to less grid feed-in “e” or to an increased grid consumption “gc”. Losses without additional labelling only lead to an increase in grid consumption. While "sby" stands for consumption in standby mode, "periph" stands for peripheral consumption. The latter includes, for example, the consumption of the current sensor, the energy manager or a consumption of the BMS which is covered from the AC side. A detailed explanation of the conversion paths can be found in points 2.4.5 and 2.4.7.

To find out which losses (L) have the largest influence on the system efficiency and the resulting total cost, the individual losses are calculated for each reference day. Based on the results they are extrapolated for the whole reference year (y) by using Eq. (5). X stands in this case as a placeholder for the different losses. The calculation methodology for the different losses is explained below.

While the electricity price in Germany is 30.46 cents/kWh (April 2019) [30], the feed-in tariff is 9.87 cents/kWh (January 2020) [31]. The calculated energetic losses can thus be translated into an annual monetary loss.

$$E_{L,X,y} = \sum_{\text{all ref.d}} (E_{L,X,d} \cdot n_{ref.d}) \quad (5)$$

2.4.3. Battery efficiency

The losses in the battery occur during both charging ($E_{L,BAT,chg}$) and discharging ($E_{L,BAT,dischg}$). To calculate these, Eqs. (6) and (9) are used. It is assumed that the efficiency during charging is the same as during discharging. However, since the amount of energy required for charging is higher, the resulting losses are higher. In order to be able to determine whether losses during battery charging and discharging lead to a higher grid consumption or a reduced grid feed-in, it must be known whether the battery is fully charged or discharged during the day, and if so, when. The corresponding method is shown in Fig. 2. The battery voltage is

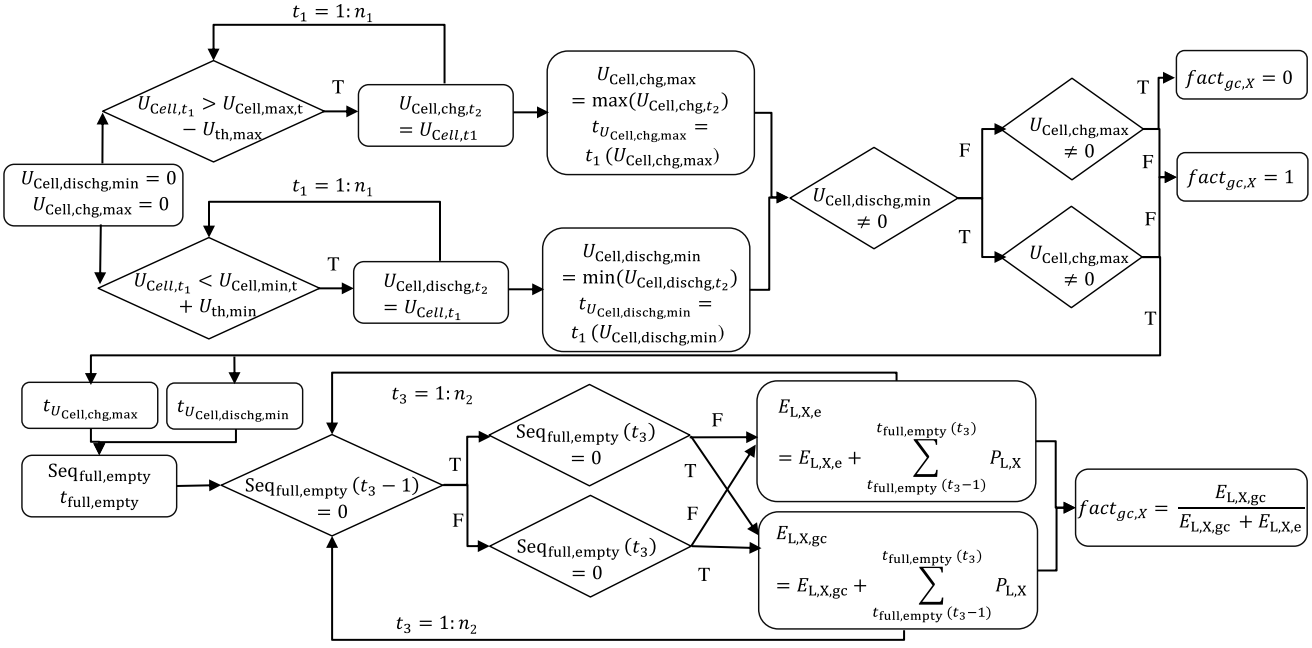

Fig. 2. Flowchart for calculating whether the battery is fully charged or discharged during the day and a grid consumption factor ($fact_{gc}$) for a certain loss during battery charging or discharging.

continuously measured and recorded during operation. Since the battery configuration of the individual systems is known, the Open Circuit Voltage (OCV) per cell can be determined as described in [6] for systems based on NMC cells. For all other cell chemistries only the single cell voltage is determined, since only incomplete measurement results are available for the internal resistance determination of all other cell chemistries. $U_{Cell,max,t}$ (see Fig. 2) is the maximum cell voltage that has occurred during the complete reference day measurements. $U_{Cell,t1}$ in contrast is the cell voltage during the course of the day. $U_{th,max}$ is determined individually for each system and varies between 0.01 V and 0.1 V depending on how much the cell voltage fluctuates when the battery is fully charged. If $U_{th,max}$ is subtracted from $U_{Cell,max,t,}$ a limit value can be determined at which the battery is still considered full. To determine whether the battery is completely discharged, the same procedure is used, except that $U_{th,min}$ is added to $U_{Cell,min,t}$ and not subtracted. $U_{Cell,chg,max}$ is the maximum cell voltage that occurs during the day being evaluated if the battery is fully charged. Therefore, $U_{Cell,chg,max}$ is changed to a value not equal to zero on days when the battery is fully charged. The same applies to a completely discharged battery and the value $U_{Cell,dischg,min}$. A grid consumption factor ($fact_{gc,X}$) is used to calculate which percentage of the respective losses lead to a higher grid consumption or to a lower grid feed-in. This factor is then multiplied with the respective losses. On days when the battery is not full, this factor is set to 1, as this energy could have been used to cover the HH load. The opposite is true for days on which the battery is only fully charged but not completely discharged. Here the respective losses only lead to a reduction in grid feed-in. Thus $fact_{gc,X}$ is set to 0. The determination is somewhat more complicated on days where both occur. Based on the knowledge of the time during the day when the battery is completely charged or discharged, a sequence $Seq_{full,empty}$ is created, which represents the fully charged and discharged states during the day. Where 0 stands for an empty battery and 1 for a fully charged one. In parallel to this, the respective time for each event is stored in the vector $t_{full,empty}$. All losses that take place between the states 1 and 0 as well as 0 and 0 lead to an increase in the grid consumption, since this energy could have been used to cover the load later. Losses that take place between the states 0 and 1 as well as 1 and 1 lead to a reduction in grid feed-in as a reduction would only lead to more energy being fed in later during the day. The $fact_{gc,X}$ is then calculated from the ratio of the losses that lead to an increase in grid consumption to the total losses. For the losses occurring during battery charging this is for example determined from the ratio between energy with which the battery is charged, which leads to an increase in the grid consumption, to the total energy with which the battery is charged during the day.

$$E_{L,BAT,chg,e,d} = \left(E_{DC,BAT,chg,d} \cdot \left(1 - \sqrt{\left(\frac{Eff_{BAT,d}}{100}\right)}\right)\right) \cdot (1 - fact_{gc,BAT,chg,d}) \tag{6}$$

$$E_{L,BAT,chg,gc,d} = \left(E_{DC,BAT,chg,d} \cdot \left(1 - \sqrt{\left(\frac{Eff_{BAT,d}}{100}\right)}\right)\right) \cdot fact_{gc,BAT,chg,d} \tag{7}$$

$$E_{L,BAT,dischg,e,d} = (E_{L,BAT,d} - E_{L,BAT,chg,d}) \cdot (1 - fact_{gc,BAT,dischg,d}) \tag{8}$$

$$E_{L,BAT,dischg,gc,d} = (E_{L,BAT,d} - E_{L,BAT,chg,d}) \cdot fact_{gc,BAT,dischg,d} \tag{9}$$

The Eqs. (6) to (9) can then be used to calculate battery losses during charging and discharging. This last part of the methodology can also be used to evaluate the losses over several days, such as the ADRES load data.

The above decribed procedure does not take into account whether the battery would have been fully charged if the losses had not occurred. The determined monetary losses may be overestimated. However, taking this issue into account is relatively complicated and would lead to more inaccuracies. Furthermore, the influence only plays a role on days with average PV production and the influence on the results is relatively limited.

2.4.4. MPP tracking losses

MPP tracking losses can be calculated acording to Eq. (10). $P_{DC,PV,t}$ is the target PV power. Some systems have very high MPP tracking efficiencies. Due to measurement inaccuracies, values greater than 100 % may be determined. To obtain more reasonable values in cases where the MPP tracking efficiency exceeds 99.9 %, the calculated MPP losses are filtered. The home storage systems are operated with a constant PV voltage for the measurements described. An average value can be calculated from the measured PV voltage values at times when the PV system generates power. To filter the power values (MPP tracking losses), it has proven to be useful to filter all power losses at times when the measured PV voltage deviates by less than 5 % from the average PV voltage.

$$P_{L,MPPT} = P_{DC,PV,t} - P_{DC,PV} \text{ if } P_{DC,PV,t} > 0 \tag{10}$$

2.4.5. Power conversion DC

According to the efficiency guideline [14], DC-coupled systems have the following three well assignable power paths: PV power conversion from DC to AC (PV2AC), battery charging (PV2BAT) and battery discharging (BAT2AC). In some systems, the path AC2BAT (battery recharging from the grid) also occurs. In addition to these pure paths, mixed operation also takes place during operation. This includes the paths PV&BAT2AC (PV feed-in with simultaneous battery discharge) and PV2BAT&AC (PV feed-in with simultaneous battery charge). To calculate the losses in real operation, the operating states are determined at any time and the losses are then assigned to the paths. The same applies to the standby states in chapter 2.4.6. Since measured values never really become zero, the individual powers are filtered to determine the operating states. This is indicated in Eqs. (11) to (34) by the suffix "f". For filtering, a moving average over 600 values (2 min) and a subsequent filtering around zero with ± 25 W has proven to be suitable for DC systems. A further reason for filtering is that often, for example for legal reasons, a light grid feed-in takes place although there is no excess power. If the measured values were not filtered, a clear assignment of the states would not be possible. Losses that occur as soon as excess PV power is fed into the grid only lead to a reduction in grid feed-in. Losses in the PV2AC path ($E_{L,PV2AC}$) as well as in the PV2BAT&AC path ($E_{L,PV2BAT\&AC}$) can therefore both lead to an increase in grid consumption (gc) (see Eqs. (12), (14) and (16)) as well as to a reduction in grid feed-in (e) (see Eqs. (11) and (13) to (15)). Whether losses of the PV2BAT&AC path actually lead to an increase of the grid consumption as long as no excess power is fed into the grid again depends on whether the battery is completely charged and or discharged on the corresponding day and when they occur. The same applies to the conversion losses of paths BAT2AC ($E_{L,BAT2AC}$) (see Eqs. (18), (21) and (22)) and PV&BAT2AC ($E_{L,PV\&BAT2AC}$) (see Eqs. (17), (19) and (20)). The method described in Section 2.4.3 is also applied here with one exception (see Eqs. (15) and (16)). On days when the battery will be both fully charged and fully discharged, the factors $fact_{gc,PV2BAT\&AC,HH,d}$, $fact_{gc,PV\&BAT2AC,d}$ and $fact_{gc,BAT2AC,d}$ represent the ratios of the losses that lead to an increase in grid consumption to the corresponding total losses of the respective path. Losses of the conversion path AC2BAT ($E_{L,AC2BAT}$) always lead to an increase in grid consumption in DC-coupled systems, since this means recharging the battery at times when no PV power is available (see Eq. (23)). An explanation of the power values and their sign convention can be found in Fig. 1.

$$E_{L,PV2AC,e,d} = \sum P_{DC,PV} + P_{AC,INV} \quad if\ P_{DC,PV,f} > 0\ \&\ P_{DC,BAT,f} = 0\ \&\ P_{AC,INV,f} < 0\ \&\ P_{Grid,f} \geq 0 \tag{11}$$

$$E_{L,PV2AC,gc,d} = \sum P_{DC,PV} + P_{AC,INV} \quad if\ P_{DC,PV,f} > 0\ \&\ P_{DC,BAT,f} = 0\ \&\ P_{AC,INV,f} < 0\ \&\ P_{Grid,f} < 0 \tag{12}$$

$$E_{L,PV2BAT\&AC,grid} = \sum P_{DC,BAT} + P_{DC,PV} + P_{AC,INV} \quad if\ P_{DC,PV,f} > 0\ \&\ P_{DC,BAT,f} < 0\ \&\ P_{AC,INV,f} < 0\ \&\ P_{Grid,f} \geq 0 \tag{13}$$

$$E_{L,PV2BAT\&AC,HH} = \sum P_{DC,BAT} + P_{DC,PV} + P_{AC,INV} \quad if\ P_{DC,PV,f} > 0\ \&\ P_{DC,BAT,f} < 0\ \&\ P_{AC,INV,f} < 0\ \&\ P_{Grid,f} < 0 \tag{14}$$

$$E_{L,PV2BAT\&AC,gc,d} = E_{L,PV2BAT\&AC,HH} \cdot fact_{gc,PV2BAT\&AC,HH,d} \tag{16}$$

$$E_{L,PV2BAT\&AC,e,d} = E_{L,PV2BAT\&AC,grid} + E_{L,PV2BAT\&AC,HH} \cdot (1 - fact_{gc,PV2BAT\&AC,HH,d}) \tag{15}$$

$$E_{L,PV\&BAT2AC,d} = \sum P_{DC,BAT} + P_{DC,PV} + P_{AC,INV} \quad if\ P_{DC,PV,f} > 0\ \&\ P_{DC,BAT,f} > 0\ \&\ P_{AC,INV,f} < 0 \tag{17}$$

$$E_{L,BAT2AC,d} = \sum P_{DC,BAT} + P_{AC,INV} \quad if\ P_{DC,PV,f} \le 0\ \&\ P_{DC,BAT,f} > 0\ \&\ P_{AC,INV,f} < 0 \tag{18}$$

$$E_{L,PV\&BAT2AC,e,d} = E_{L,PV\&BAT2AC,d} \cdot (1 - fact_{gc,PV\&BAT2AC,d}) \tag{19}$$

$$E_{L,PV\&BAT2AC,gc,d} = E_{L,PV\&BAT2AC,d} \cdot fact_{gc,PV\&BAT2AC,d} \tag{20}$$

$$E_{L,BAT2AC,e,d} = E_{L,BAT2AC,d} \cdot (1 - fact_{gc,BAT2AC,d}) \tag{21}$$

$$E_{L,BAT2AC,gc,d} = E_{L,BAT2AC,d} \cdot fact_{gc,BAT2AC,d} \tag{22}$$

$$E_{L,AC2BAT,d} = \sum P_{AC,INV} + P_{DC,BAT} \quad if\ P_{DC,PV,f} \le 0\ \&\ P_{DC,BAT,f} < 0\ \&\ P_{AC,INV,f} > 0 \tag{23}$$

$$E_{L,MPPT,grid} = \sum P_{L,MPPT} \quad if\ P_{DC,BAT,f} \le 0\ \&\ P_{AC,INV,f} < 0\ \&\ P_{Grid,f} \ge 0 \tag{24}$$

$$E_{L,MPPT,HH} = \sum P_{L,MPPT} \quad if\ P_{AC,INV,f} < 0\ \&\ (P_{Grid,f} < 0\ \|\ P_{DC,BAT,f} \le 0) \tag{25}$$

$$E_{L,MPPT,e,d} = E_{L,MPPT,grid} + E_{L,MPPT,HH} \cdot (1 - fact_{gc,MPPT,HH,d}) \tag{26}$$

$$E_{L,MPPT,gc,d} = E_{L,MPPT,HH} \cdot fact_{gc,MPPT,HH,d} \tag{27}$$

2.4.6. Standby DC

In DC-coupled systems, standby consumption, whether it occurs on the AC side or at the PV input on the DC side, always leads to an increase of grid consumption (see Eqs. (30) and (31)). Standby consumption at the battery input of the DC side can again lead to both, an increase of grid consumption as well as a reduction in grid feed-in. This also depends on whether the battery is completely charged or discharged during the day. The procedure described in Section 2.4.3 and Section 2.4.5 is applied for the determination. In DC-coupled systems, standby consumption, whether it occurs on the AC side or on the DC side, always leads to an increase of grid consumption (see Eqs. (28) to (31)). The consumption of peripheric components is not separately measured, but can be determined from the three sensors $P_{AC,INV}$, P_{Load} and P_{Grid}. As long as excess power is fed into the grid and the battery is not discharged, the consumption of peripheric components only leads to a reduced grid feed-in.

2.4.7. Power conversion AC

AC systems have three conversion paths: battery charging (AC2BAT), battery discharging (BAT2AC) and PV power conversion from DC to AC (PV2AC).The losses occurring in the paths can lead to a higher grid consumption as well as to a reduced grid feed-in. For the losses of the PV2AC path, this can be determined by the PV power fed into the grid ($P_{GRID,PV}$) (see Eqs. (40) and (41)). As soon as PV power is fed into the grid, losses during power conversion only lead to a lower grid feed-in. For better comprehensibility, a part of the loss calculation is represented by a flowchart (see Fig. 3). Here, (T) means true and (F) means false. The calculation of $P_{GRID,PV}$ as well as the total AC power supplied by PV ($P_{AC,CONS,PV}$) is represented by Fig. 3. For the same reason as for DC-coupled systems, $P_{GRID,PV}$ needs to be filtered to determine whether PV excess power is fed into the grid or not. This is respectively indicated by the suffix "f" for filtered (see Eqs. (40) and (41)). For filtering, a moving average over 600 values (2

$$E_{sby,DC,BAT,e,d} = (\sum P_{DC,BAT}) \cdot (1 - fact_{gc,sby,DC,BAT,d}) \quad if\ P_{DC,BAT,f} > 0\ \&\ P_{AC,INV,f} \ge 0 \tag{28}$$

$$E_{sby,DC,BAT,gc,d} = (\sum P_{DC,BAT}) \cdot fact_{gc,sby,DC,BAT,d}) \quad if\ P_{DC,BAT,f} > 0\ \&\ P_{AC,INV,f} \ge 0 \tag{29}$$

$$E_{sby,DC,PV,d} = \sum P_{DC,PV} \quad if\ P_{DC,BAT,f} \ge 0\ \&\ P_{AC,INV,f} \ge 0 \tag{30}$$

$$E_{sby,AC,INV,d} = \sum P_{AC,INV} \quad if\ P_{DC,BAT,f} \ge 0\ \&\ P_{AC,INV,f} \ge 0 \tag{31}$$

$$E_{periph,d} = \sum P_{Grid} + P_{AC,INV} + P_{Load} \tag{32}$$

$$E_{periph,e,d} = \sum P_{Grid} + P_{AC,INV} + P_{Load} \quad if\ P_{Grid,f} \ge 0\ \&\ P_{DC,BAT,f} < 0\ \&\ P_{DC,PV,f} > 0 \tag{33}$$

$$E_{periph,gc,d} = E_{periph,d} - E_{periph,e,d} \tag{34}$$

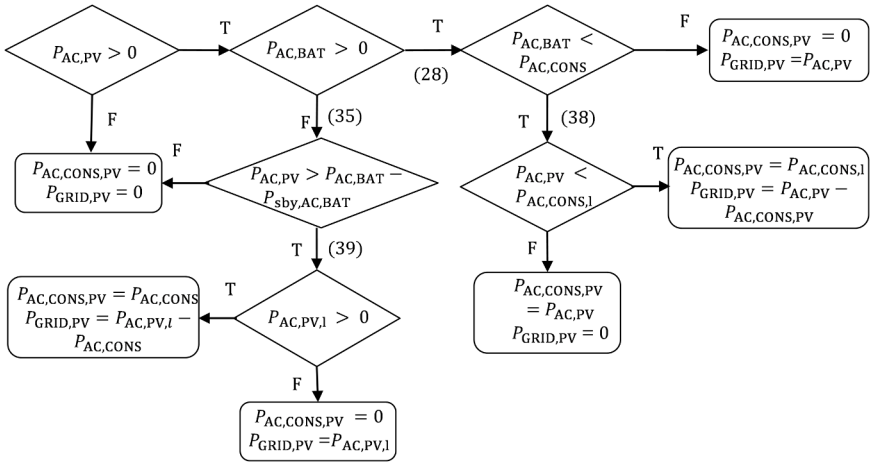

Fig. 3. Flowchart of the calculation of the total AC power ($P_{AC,CONS,PV}$) supplied by PV and of the excess PV power ($P_{GRID,PV}$).

min) and subsequent filtering around zero with ± 75 W for AC systems has proven suitable.

The decision criterion for AC2BAT ($E_{L,AC2BAT,d}$) as well as BAT2AC ($E_{L,BAT2AC,d}$) conversion losses is exactly the same as for battery losses during battery charging. Here, as well, the decision depends on whether or not the battery becomes fully charged and or completely discharged on the corresponding day. For the determination the procedure described in Section 2.4.3 and Section 2.4.5 as well as Eqs. (42) to (47) are used.

$$P_{sby,AC,BAT} = P_{AC,BAT} \quad if\ P_{AC,BAT} < 0\ \&\ P_{DC,BAT} \le 0 \tag{35}$$

$$P_{periph} = P_{Grid} + P_{SYS} + P_{Load} \tag{36}$$

$$P_{AC,CONS} = P_{LOAD} + P_{sby,AC,BAT} + P_{periph} \tag{37}$$

$$P_{AC,CONS,l} = P_{AC,CONS} - P_{AC,BAT} \tag{38}$$

$$P_{AC,PV,l} = P_{AC,PV} - P_{AC,BAT} - P_{sby,AC,BAT} \tag{39}$$

$$E_{L,PV2AC,e,d} = \sum P_{DC,PV} - P_{AC,PV} \quad if\ P_{GRID,PV,f} \ge 0 \tag{40}$$

$$E_{L,PV2AC,gc,d} = \sum P_{DC,PV} - P_{AC,PV} \quad if\ P_{DC,PV} > 0\ \&\ P_{AC,PV} > 0\ \&\ P_{GRID,PV,f} < 0 \tag{41}$$

$$E_{L,BAT2AC,d} = \sum P_{DC,BAT} - P_{AC,BAT} \quad if\ P_{DC,BAT} > 0\ \&\ P_{AC,BAT} > 0 \tag{42}$$

$$E_{L,AC2BAT,d} = \sum P_{AC,BAT} - P_{DC,BAT} \quad if\ P_{DC,BAT} < 0\ \&\ P_{AC,BAT} < 0 \tag{43}$$

$$E_{L,BAT2AC,e,d} = E_{L,BAT2AC,d} \cdot (1 - fact_{gc,BAT2AC,d}) \tag{44}$$

$$E_{L,BAT2AC,gc,d} = E_{L,BAT2AC,d} \cdot fact_{gc,AC2BAT2AC,d} \tag{45}$$

$$E_{L,AC2BAT,e,d} = E_{L,AC2BAT,d} \cdot (1 - fact_{gc,AC2BAT,d}) \tag{46}$$

$$E_{L,AC2BAT,gc,d} = E_{L,AC2BAT,d} \cdot fact_{gc,AC2BAT,d} \tag{47}$$

$$E_{L,MPPT,grid} = \sum P_{L,MPPT} \quad if\ P_{DC,PV,t} > 0\ \&\ P_{GRID,PV,f} \ge 0 \tag{48}$$

$$E_{L,MPPT,HH} = \sum P_{L,MPPT} \quad if\ P_{DC,PV,t} > 0\ \&\ P_{GRID,PV,f} < 0 \tag{49}$$

$$E_{L,MPPT,e,d} = E_{L,MPPT,grid} + E_{L,MPPT,HH} \cdot (1 - fact_{gc,MPPT,HH,d}) \tag{50}$$

$$E_{L,MPPT,gc,d} = E_{L,MPPT,HH} \cdot fact_{gc,MPPT,HH,d} \tag{51}$$

2.4.8. Standby AC

In AC systems, standby consumption can occur on both the AC and the DC side of the PV as well as of the battery inverter. Standby consumption on the DC side of the PV inverter leads to an increased grid consumption. While standby consumption on the DC side means that the PV power is no longer available to cover the load and thus increases grid consumption, AC standby consumption of the PV inverter directly leads to a higher grid consumption. Standby consumption on the DC side of the battery inverter can again lead to both an increase of grid consumption as well as a reduction in grid feed-in. This again depends on whether the battery is completely charged or discharged during the day and when the standby consumption occurs. The procedure described in Section 2.4.3 and Section 2.4.5 is applied for the determination. Standby consumption on the AC side of the battery inverter and consumption of peripheral components can lead to both reduced grid feed-in and higher grid consumption, depending on whether they are covered by PV power or not. The way to determine the coverage by PV or grid is represented by Fig. 4 and Eqs. (52) to (61). It is assumed that the PV power first covers the HH load (P_{Load}), then the standby consumption on the AC side of the battery inverter ($P_{sby,AC,BAT}$) and then the consumption of all peripheral components (P_{periph}).

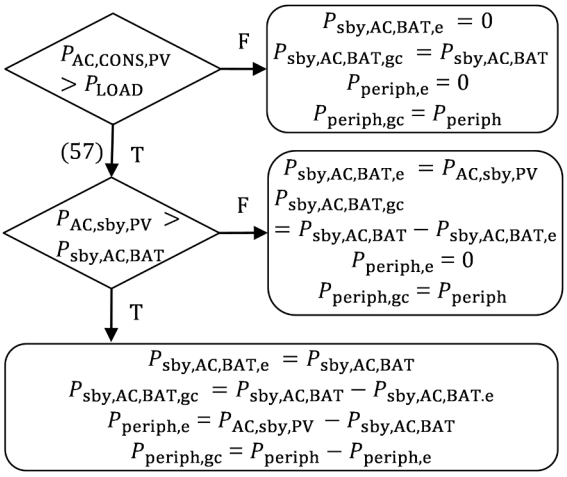

Fig. 4. Flowchart of the calculation of the AC standby power of the battery ($P_{AC,sby,BAT}$) and the peripheral consumption (P_{periph}), both either supplied by PV (e) or the grid (gc).

$$E_{sby,DC,PV,d} = \sum P_{DC,PV} \quad if\ P_{DC,PV} > 0\ \&\ P_{AC,PV} < 0 \tag{52}$$

$$E_{sby,AC,PV,d} = \sum P_{AC,PV} \quad if\ P_{DC,PV} > 0\ \&\ P_{AC,PV} < 0 \tag{53}$$

$$E_{sby,DC,BAT,d} = \sum P_{DC,BAT} \quad if\ P_{DC,BAT} > 0\ \&\ P_{AC,BAT} < 0 \tag{54}$$

$$E_{sby,DC,BAT,e,d} = E_{sby,DC,BAT,d} \cdot (1 - fact_{gc,sby,DC,BAT,d}) \tag{55}$$

$$E_{sby,DC,BAT,gc,d} = E_{sby,DC,BAT,d} \cdot fact_{gc,sby,DC,BAT,d} \tag{56}$$

$$P_{AC,sby,PV} = P_{AC,CONS,PV} - P_{Load} \tag{57}$$

$$E_{sby,AC,BAT,gc,d} = \sum P_{AC,BAT,gc} \tag{58}$$

$$E_{sby,AC,BAT,e,d} = \sum P_{AC,BAT,e} \tag{59}$$

$$E_{periph,gc,d} = \sum P_{periph,gc} \tag{60}$$

$$E_{periph,e,d} = \sum P_{periph,e} \tag{61}$$

3. Results of measurement and analysis

3.1. Total system efficiency

The efficiency of the entire home storage system over the course of a synthetic year can be determined from the reference day measurements (see test 1 in Table 3) using Eq. (3). Fig. 5 displays the results of 12 home storage systems: the system efficiencies (including losses from the PV inverter in the case of AC-coupled systems) are between 81.9 % and 94.1 %. Note that the system efficiency refers to the efficiency of the entire system, where losses due to direct use of PV power (both self-consumption and grid feed-in) have been taken into account. It is evident from Fig. 5, that there are major differences between the systems. In order to verify that similar system efficiencies are also achieved with different load data, further measurements with load data from the "ADRES-CONCEPT" project were carried out (see "test 2" in Table 3). The resulting efficiencies are shown in Fig. 5 on the right: The system efficiencies of VDI winter and summer days are compared with the corresponding results of the 9 different ADRES HH. The results were calculated using Eq. (4). In both measurements the same PV data was used. The min and max values of the errorbars (Fig. 5 right panel) show the min and max values determined for the 9 ADRES HH. In each case the mean value is represented by the dot in the same colour as the bars. For all storage systems the results of the reference days lie within the range of the results of the ADRES HH, in most cases they are even closer to the mean value. Thus it can be stated that the reference day measurements are quite representative with regard to system efficiency. The complete data set of 9 ADRES HH is available for all systems except system C (2) and L (6).

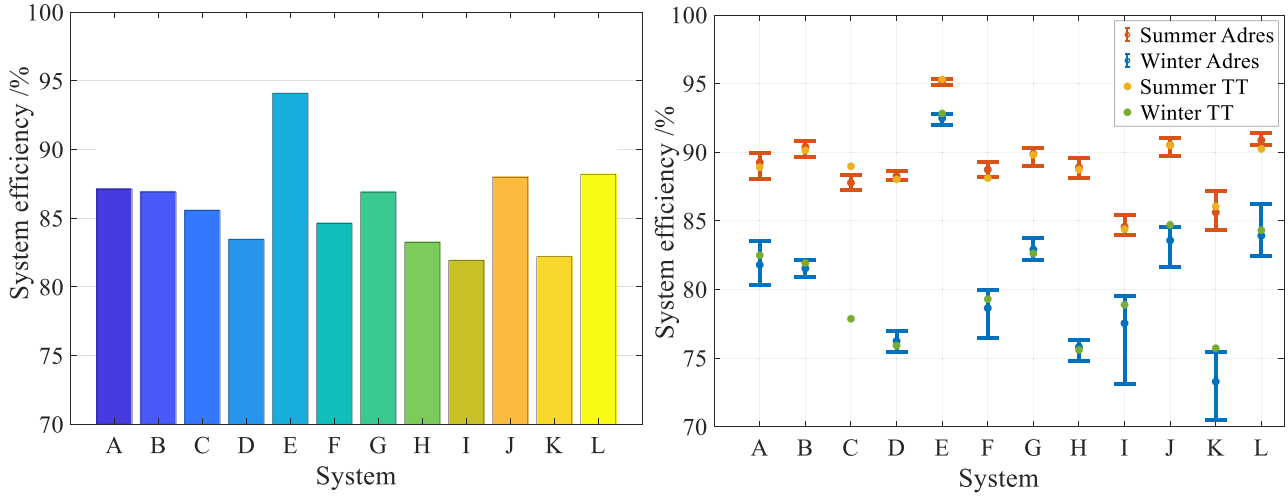

Fig. 5. Comparison of the total system efficiencies for the systems A to L, measured for a reference five-person household with an annual electricity consumption of 4200 kWh.

High system efficiency is primarily achieved on days with high irradiation (for example clear summer days), since in this case the power electronics operate in a high-efficiency range, which directly effects the efficiency as a whole (see [8] and Fig. 5 right panel). For this reason, efficiencies are always higher in summer (in the northern hemisphere) than in winter. Munzke et al. [8] also mention that efficiencies on holidays/Sundays might be slightly higher than those of weekdays, since more PV energy is directly consumed rather than having to be stored for later use, reducing the losses due to energy conversion.

System efficiency is mainly influenced by losses due to conversion efficiency, battery efficiency and standby consumption. Furthermore, system sizing has an influence on system efficiency. Above all the usable battery capacity and the size of the power electronics, and their relation to the load and generation power profiles. The different aspects will be more closely examined in the following sections.

3.2. Influence of battery efficiency and capacity (system sizing) on the total system efficiency

The battery efficiency of the systems varies between 78.4 % and 99.0 % for the reference year (see Fig. 6 left panel). The very low battery efficiency of 78.4 % is due to the fact that a DCDC inverter is integrated in the battery itself. The corresponding battery efficiencies of the ADRES HH are shown in the right panel of Fig. 5. Again, a large overlap of the results of the VDI reference summer and winter days and the ADRES HH is observed.

It is interesting to note that there is no noticeable effect of usable battery capacity on battery efficiency (see Fig. 7 upper panel), which is due to the fact that batteries within households are operated at a relatively low power or C-rate. For both the reference household and the ADRES HH, the C-rate is between 0.08C and 0.41C for charging and 0.03C and 0.30C for discharging, depending on the strorage system. A more detailed analysis has been done in a previous paper of the authors [8]. Furthermore, cycle tests according to the efficiency guidelines revealed that for most of the systems, the influence of the magnitude of the charge and discharge powers on the battery efficiency has a similar effect: the smaller the power value, the larger the battery efficiency [8].

The usable battery capacity however influences the energy charged and discharged within the battery during one year, as shown in the panel in the center of Fig. 7. Nevertheless the energy losses and the resulting economic losses mainly depend on the efficiency of the battery and not on its capacity (see Fig. 8). Thus no functional correlation can be observed in the lower panel of Fig. 6. The influence of the efficiency of the batteries on battery losses occuring in real operation is therefore

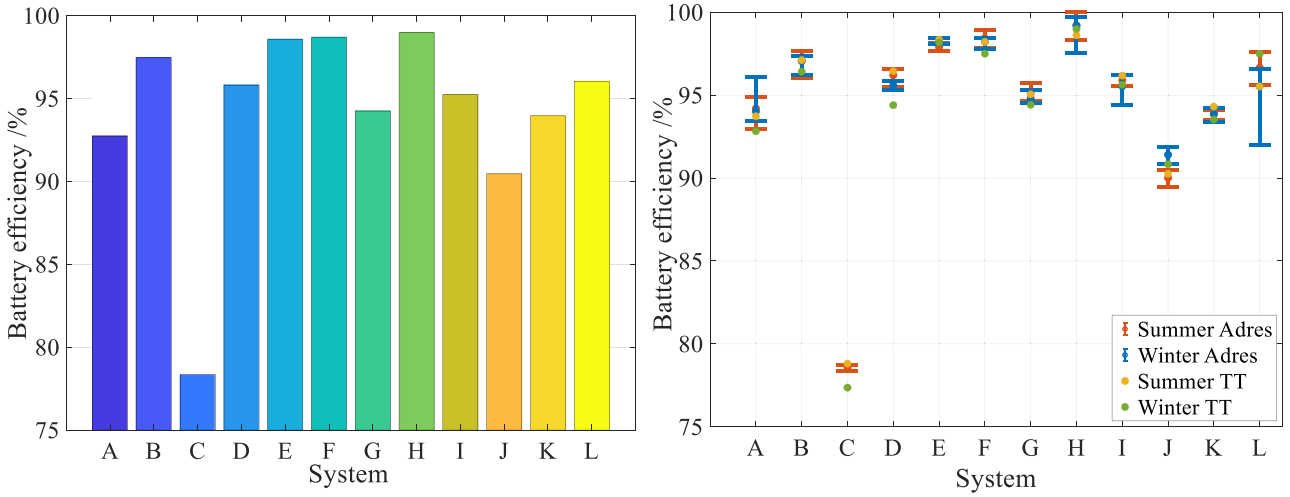

Fig. 6. Comparison of the battery efficiencies for the systems A to L, measured for a reference five-person household with an annual electricity consumption of 4200 kWh.

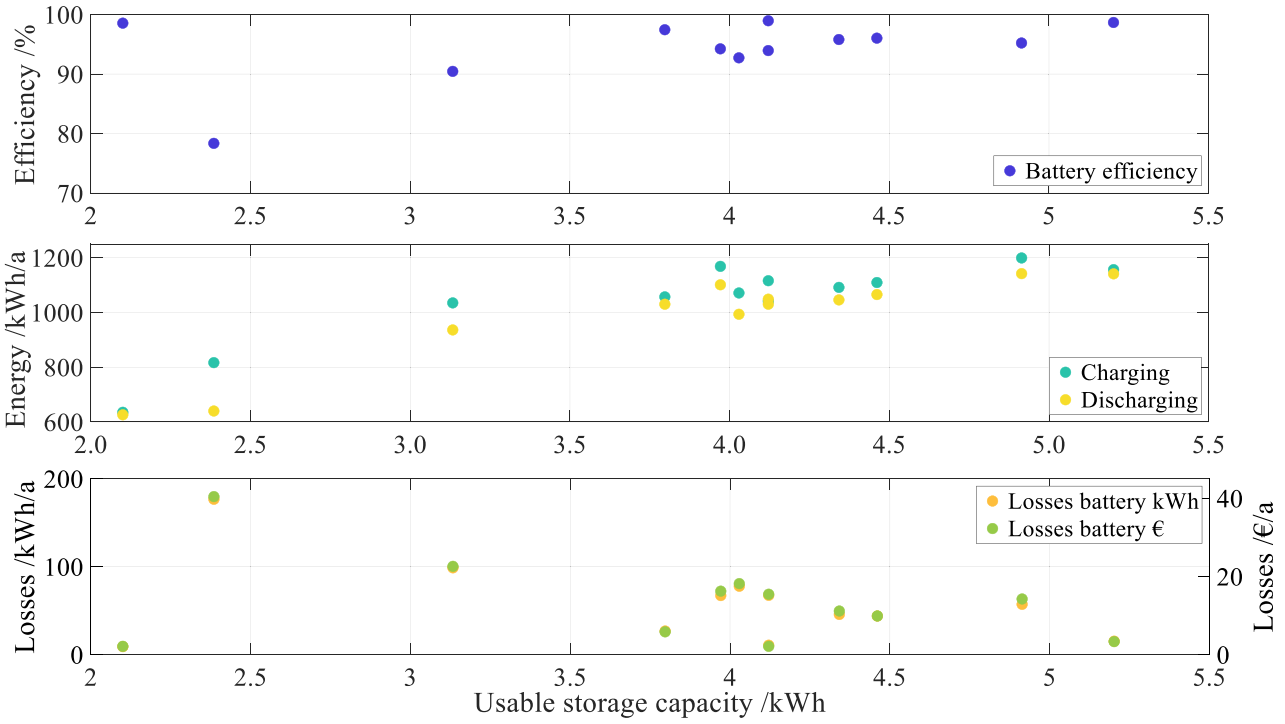

Fig. 7. Losses in €/a as a function of the useable storage capacity, the energy charged and discharged during one year and the battery efficiency.

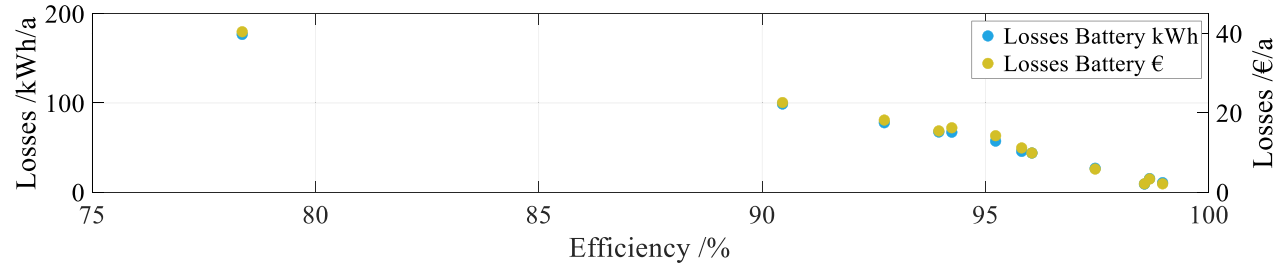

Fig. 8. Battery losses of the reference year according to VDI 4655 as a function of battery efficiency for the systems A to L.

much greater than the influence of the capacity of the batteries.

Apart from the quality of the cells themselves, the battery efficiency is to a large extent influenced by the amount of power the battery management system (BMS) requires and whether it is powered out of the battery itself. In addition, the general layout of the battery affects its efficiency. However, a detailed analysis of these influencing factors was not subject of the present study.

The monetary losses per year for the systems under test range from €2 to €40 and are calculated according to Eqs. (6)–(9).

3.3. Influence of individual power flow path efficiencies and yearly power flow distributions

Fig. 9 (left panel) shows the energy losses of the different power conversion paths for the 12 different home storage systems under evaluation determined according to Eqs. (11) to (23) for DC systems and (40) to (44) for AC systems. It is evident that there are very large differences between the systems. The differences are particularly high in the cases of charging and discharging. The energy losses of the best system regarding conversion efficiency are 72.9 % lower than the losses of the worst system. The difference is even greater for monetary losses, with 76.0 %. Already the conversion losses of the paths PV2AC and PV2BAT&AC are as high in system I as the total conversion losses of 7 of the systems. Best performing in the comparison is a DC coupled system. At the same time, the worst performing systems are also DC coupled systems. Most AC-coupled systems are in the better midfield. This suggests that DC-coupled systems can be more efficient, however, the quality of the systems is very important. The amount of energy charged to or discharged from the battery is only 15 % to 30 % of the amount of energy converted by the PV inverter, depending on the system. Nevertheless, the sum of the energy losses during battery charging and discharging is higher than the losses of the PV power conversion. This can be observed quite well, for AC-coupled systems.

As described, not all energy losses lead to equally high monetary losses. As can be seen in Table 5 and Fig. 9, there are shifts between energy and monetary losses concerning the impact of the individual losses on total losses. Losses that account for a high proportion of the system's total conversion losses (both energetic and monetary) per year are highlighted in red. In contrast, the losses with the least influence are highlighted in green. While, for example, the losses of the PV2AC and PV2BAT&AC paths make up the largest proportion of energy losses in most of the systems studied, their share of monetary losses is significantly lower for most systems. This shift is the main reason why the systems J and L change their position in the ranking (see Fig. 9). The shift is caused by the fact that some losses lead to a reduction in grid feed-in while others lead to increased grid consumption. In PV home storage systems, the batteries are discharged mostly at night. On many days this results in an empty battery. The losses lead to an increase in

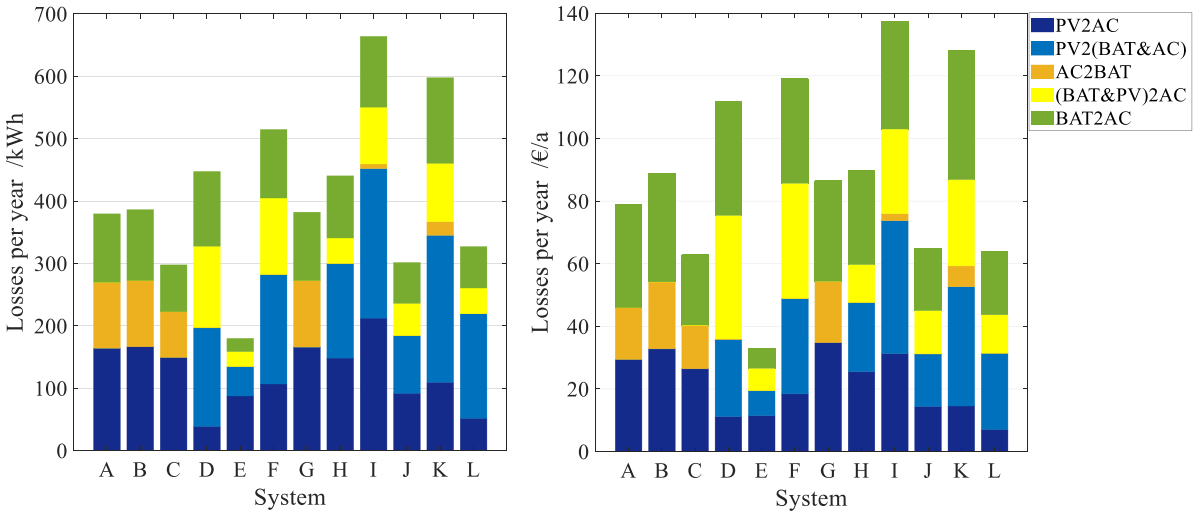

Fig. 9. Energy (left) and monetary (right) losses of the power conversion paths for a reference year according to VDI 4655 for the systems A to L.

grid consumption, since the electricity can no longer be used to cover the household load. On the other hand, the charging process is followed by a full battery during the day on many days, especially in the summer months. The losses that occur here therefore only lead to a reduction in grid feed-in. Thus, similarly high energy conversion losses during charging and discharging lead to significantly lower monetary losses from the discharging process than from the charging process (see Table 5 and Fig. 9). The annual total losses due to conversion losses range between €33 and €137.

Table 5
Comparison of the energy and monetary losses of the reference year due to power conversion of the different conversion paths (system A to L).

	Losses kWh/a					Losses €/a				
System	PV2AC	PV2BAT&AC	AC2BAT	BAT&PV2AC	BAT2AC	PV2AC	PV2BAT&AC	AC2BAT	BAT&PV2AC	BAT2AC
A	164.1	0.0	105.6	0.0	109.6	29.4	0.0	16.5	0.0	33.0
B	166.3	0.0	106.2	0.0	113.6	32.8	0.0	21.4	0.0	34.5
C	149.2	0.0	73.4	0.0	75.1	26.4	0.0	14.0	0.0	22.4
D	38.9	157.8	0.8	130.2	119.7	11.2	24.6	0.2	39.4	36.4
E	87.6	47.3	0.0	23.9	21.1	11.5	8.0	0.0	7.0	6.4
F	106.8	175.5	0.2	122.4	109.8	18.4	30.5	0.0	36.7	33.4
G	165.9	0.0	106.5	0.0	109.7	34.8	0.0	19.5	0.0	32.2
H	148.3	151.7	0.0	40.7	99.5	25.5	22.1	0.0	12.0	30.2
I	212.3	239.6	7.5	91.1	113.4	31.3	42.4	2.3	27.0	34.5
J	91.9	92.3	0.3	51.6	65.3	14.4	16.7	0.1	13.7	19.9
K	109.5	235.5	21.9	93.5	137.0	14.6	38.1	6.7	27.5	41.2
L	51.8	167.6	0.0	41.1	66.3	7.1	24.4	0.0	12.2	20.2

Comparison of the path flow efficiencies battery charging and discharging (see PV2BAT and BAT2AC in the left and right panels of Fig. 10, respectively) clearly shows that the systems show a large variation in efficiency particularly under partial load. For powers above 60 % of the nominal power the charging efficiencies range from 8.1 to 7.4 percentage points, whereas the discharging efficiencies range from 6.7 to 5.2 percentage points.

A similar picture was already described in a previous work for the power conversion pathway PV2AC (direct feed-in of PV power) – the efficiencies at loads below 40 % of the inverter's nominal power are markedly more spread than at loads above this power level [8].

In order to better understand the influence of the path flow efficiencies on the overall conversion efficiencies, it is useful to plot the efficiency curves against the output power of each specific power conversion pathway. If one in addition compares the distributions of the energy flows at different battery charge and discharge powers over a synthetic year, it is evident that a major proportion of the power flows lies below 1 kW. This ratio is significantly higher for discharging (see Fig. 11) than for charging (see Fig. 12). In the current case 44 % and 72 % of the energy used to charge the battery and between 79 % and 100 % of the energy drawn from the battery flows at powers below 1 kW. This serves to further emphasise the importance of partial load efficiencies for the overall system efficiency.

The system E that shows the lowest conversion efficiency losses over a synthetic year (see Fig. 9) shows the highest charge and discharge efficiencies throughout the entire power spectrum, as to be expected. At the same time the systems L and J show the second and third lowest conversion efficiency losses. System L has the second highest measured charging efficiency below approximately 1.0 kW for charging and below 0.5 kW for discharging. Above 1 kW, the charging efficiency of system J and L are in the same range. The systems F, I and K with the highest conversion losses (see Fig. 9) have the smallest charge and discharge efficiencies throughout the entire power spectrum.

As a consequence of the context described above it is clear that the achievable system efficiencies do not only depend on the power electronic components and their efficiencies, but also on the load and PV generation profiles over the course of the year. To further demonstrate the importance of partial load efficiencies, Fig. 13 (left panel) shows the accumulated energy flows for the reference year as a function of the nominal power of the systems. The lower the curve of the systems, the smaller the systems and the higher their utilization at a high nominal power. Values above 1 mean that the system is operated in the overload range. This is usually only possible for a limited time. In comparison, the right panel of Fig. 13 shows the power up to which 80 % of the energy is discharged from the battery. The analysis includes both the reference days as well as the ADRES HH profiles. The mean values lie between 1 and 2 kW for both summer and winter day.

In addition, an analysis of the residual power (difference between load and PV power) shows that a large proportion of the potential

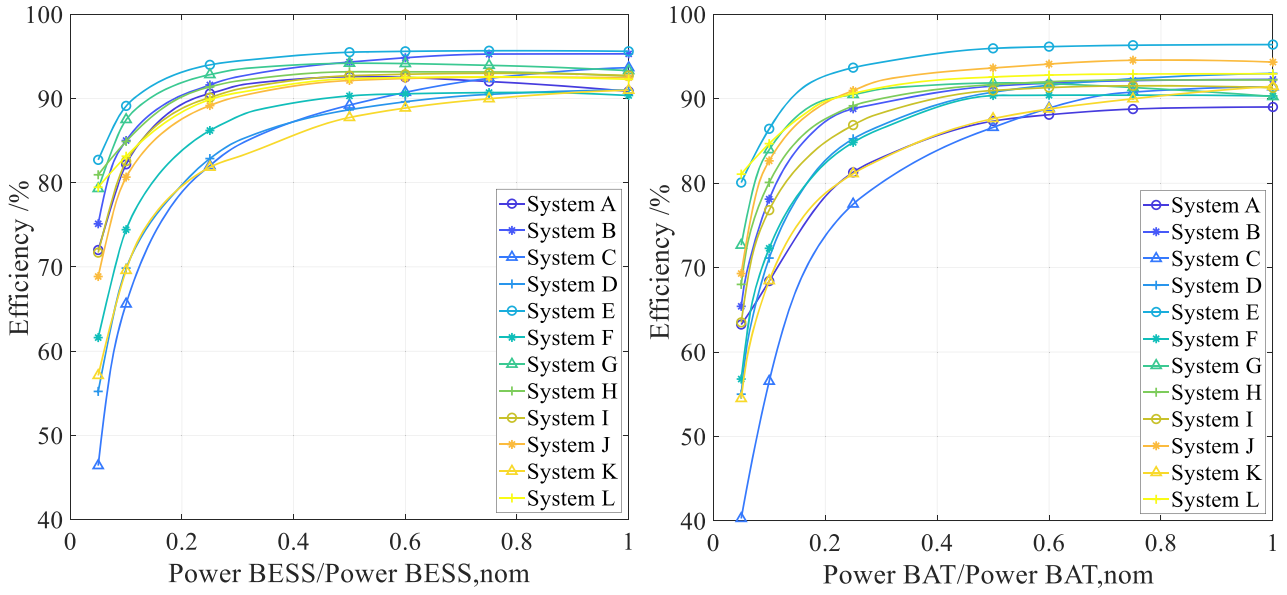

Fig. 10. Efficiency of the power conversion pathways and BAT2AC (battery discharging - left) PV2BAT (battery charging - right) as a function of the output power, for systems A to L.

discharge powers (positive values) lie between 0 kW and 1 kW, whereas the potential charge powers (negative values) are more evenly distributed. The analysis was carried out for the 9 ADRES HH with an extrapolated annual consumption of between 2975 kWh and 5399 kWh (see Fig. 14). For the load distribution over the course of the year, both the summer and winter week were assumed as load for 6 months each. The size of the PV system for this study varied between 3.5 kWp and 6.5 kWp. A larger PV system increases the charging powers, which at the same time means that the batteries would be fully charged earlier in the day on sunny summer and transition days. The fact that the charging losses for the reference days considered in this paper are only slightly lower than the discharging losses (see Table 5 and Fig. 9), although the energy distribution during charging is much more even (see Fig. 12), is related to the fact that the PV system has only 3.5 kWp. With a larger PV system, the distribution of the charging power also shifts towards a higher power.

As mentioned for the households in this study, a large proportion of the load lies under 1 kW. More precisely, between 73.7 % and 75.4 % (66.2 % and 68.3 %) of the households' consumption occurs at a power smaller than 1.5 kW (1 kW). As a consequence, it is advantageous for storage systems in household applications to be optimised in terms of their efficiency at partial load for the pathway BAT2AC (battery discharge). A larger PV system hardly changes this proportion. A similar analysis for the reference day measurements from test 1 was already published by Munzke et al. [8]. The evaluation showed similar results.

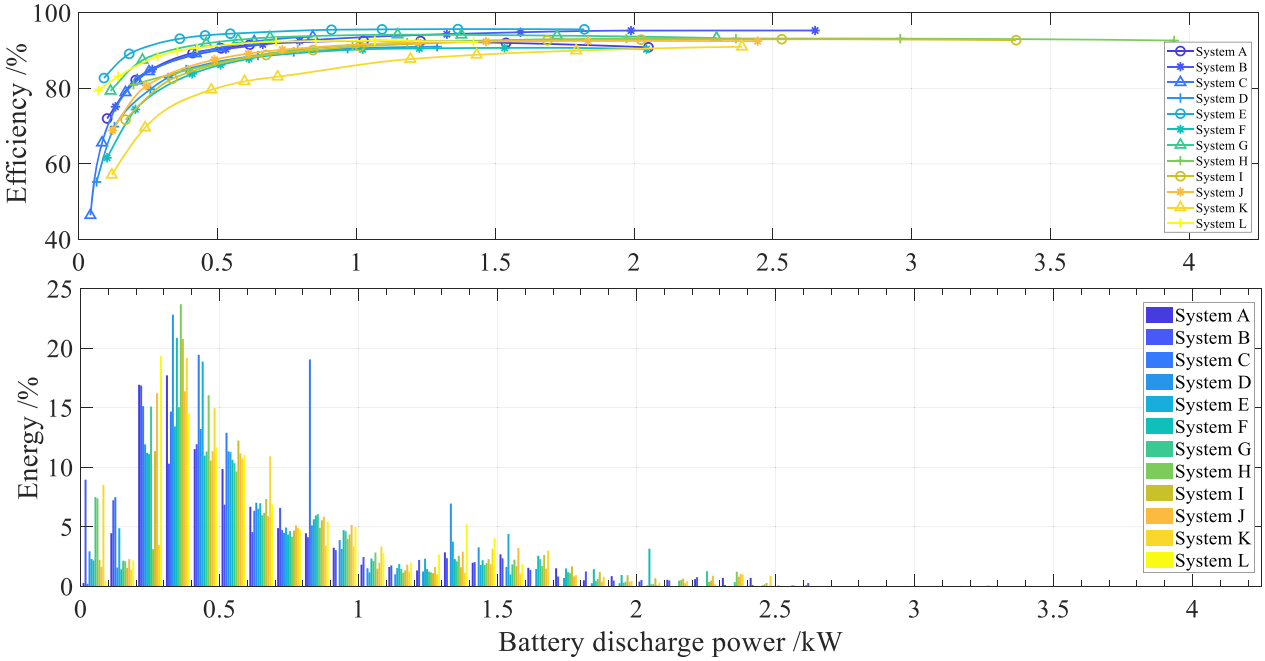

Fig. 11. Efficiency of the power conversion pathway BAT2AC (battery discharging) as a function of the input power (upper panel), as compared to the battery discharge power distribution over a synthetic year, for systems A to L.

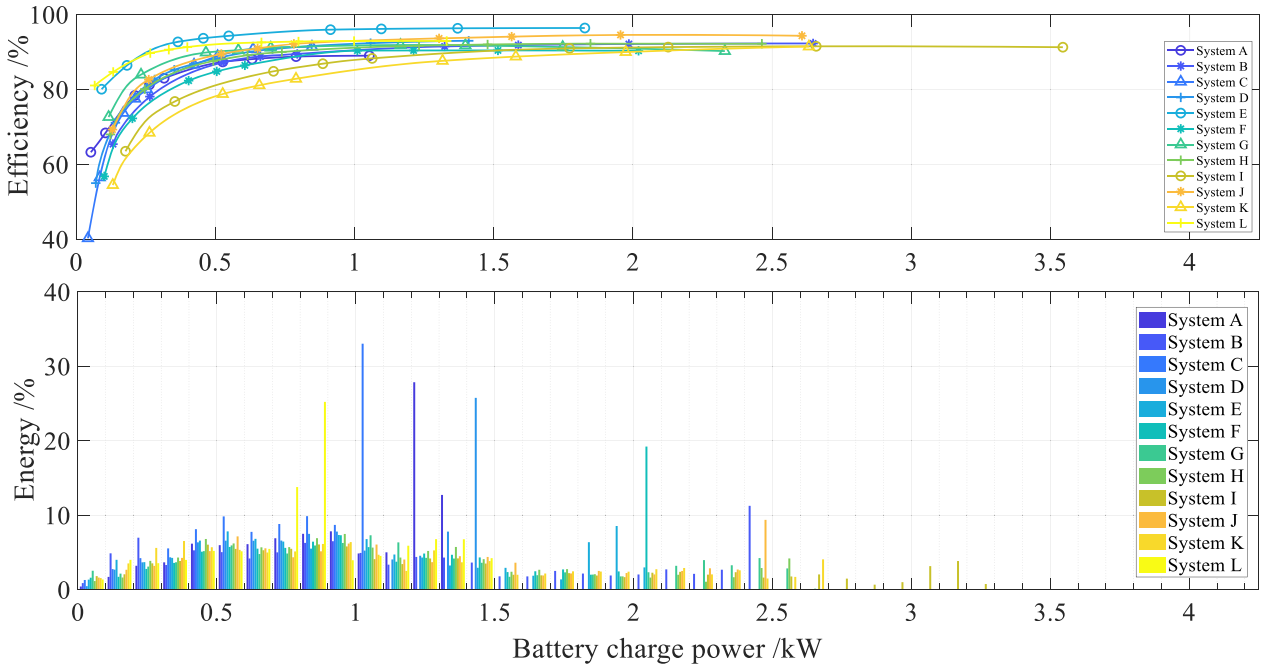

Fig. 12. Efficiency of the power conversion pathway PV2BAT (battery charging) as a function of the output power (upper panel), as compared to the battery charge power distribution over a synthetic year, for the systems A to L (lower panel).

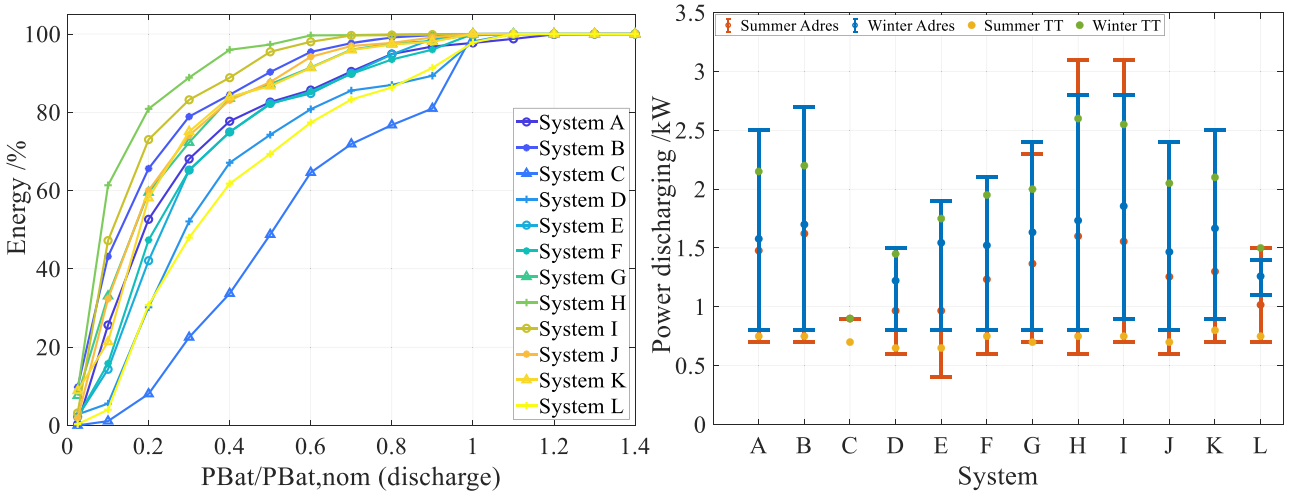

Fig. 13. Accumulated energy flows for the reference year as a function of the nominal power of the systems (left) - Power up to which 80 % of the energy is discharged from the battery of the systems A to L (right).

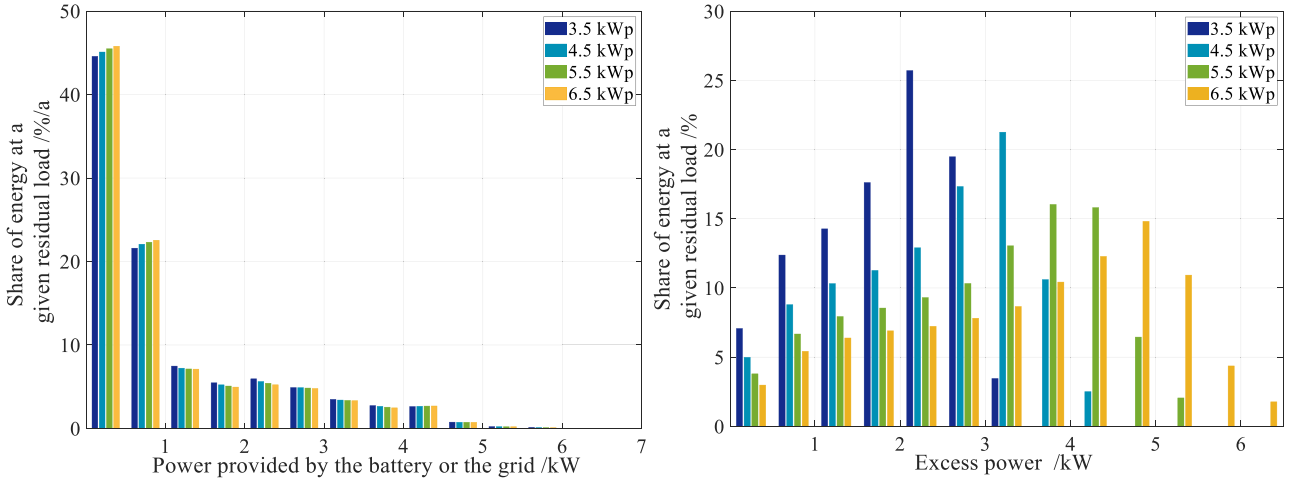

Fig. 14. Residual power distribution of the 9 households of test 2.

3.4. Standby losses

Besides the effects of losses along the power conversion pathways one also needs to take into account the effect of standby consumption on storage system performance.

The measurements performed according to the criteria in test 1 were used to extrapolate the energy drawn from the grid for a synthetic year: the monetary losses due to standby consumption work out to be between €1 and €46 per year (see Fig. 15). The calculation was done according to Eqs. (28) to (31) for DC-coupled systems and (52) to (59) for AC-coupled systems.

consumption for the systems under test varies between 0 W and 40.8 W with a full battery and between 0.1 W and 46.2 W with an empty battery (see Fig. 9 left panel).

Furthermore, consumption occurs through so-called peripheric components on the AC side of the storage systems. As mentioned above, these include for example, the consumption of the current sensor, the energy manager or a consumption of the BMS which is covered from the AC side. The required power of each system is shown in Fig. 16 in the right panel. The extrapolated losses for one year, which were determined using the reference day measurements, are shown in Fig. 17. They are labeled as PACperiph.

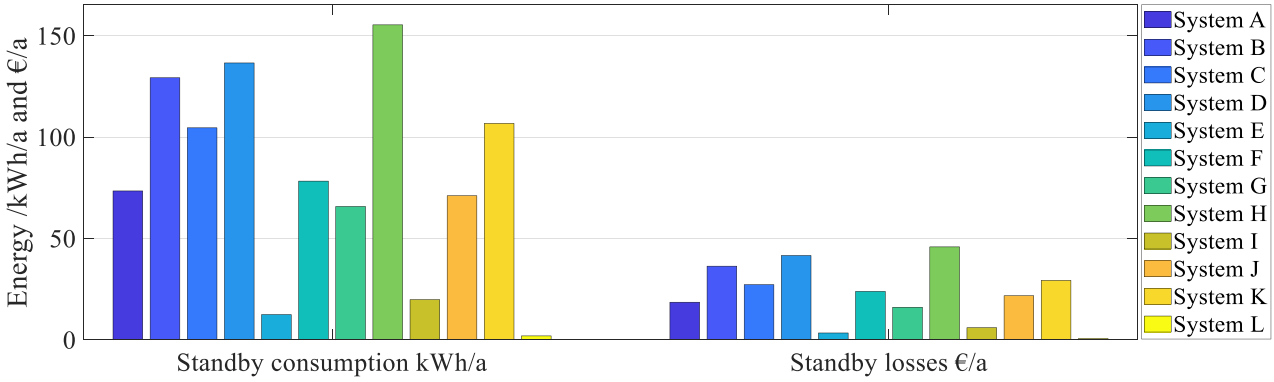

Fig. 15. Consumption (kWh) of the systems A to L in standby mode extrapolated for a year according to the VDI 4655 standard (left), yearly losses in standby mode (€) (right).

In order to accurately determine the standby power it was measured according to the efficiency guidline. As can be seen in Fig. 16, the systems have widely varying standby consumption. Standby consumption occurs either when the battery is full or empty.The required power is either provided by the battery (DC) or drawn from the grid (AC). Thus it can be divided in DC and AC standby power. A breakdown of the annual standby losses into AC and DC standby losses is shown in Fig. 17. In some systems the battery is decoupled from the power electronics in standby mode, preventing further discharge and to reduce standby consumption on the DC side of the storage system. Standby

3.5. Total losses

The measurements with reference profiles allow the energy losses to be precisely determined for one year and also to assigne them to the specific categories. In total the systems show losses of 265 kWh-974 kWh per year (incl. MPP efficiency losses) (see Fig. 17 left panel). The resulting monetary losses vary between 44 €- 238 € per year. They are shown in the right panel of Fig. 17. There are very large differences between the systems. The results clearly show the potential for improvement of the individual systems. However, the largest energy and

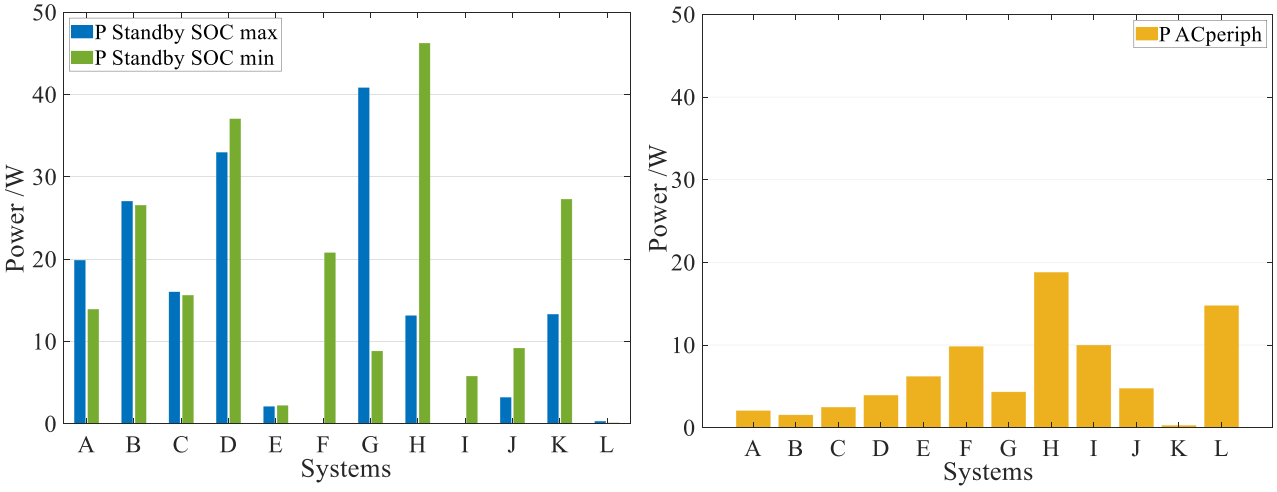

Fig. 16. Standby consumption (kW) of the systems A to L measured when the battery was completely charged or discharged (left), peripheral consumption (right).

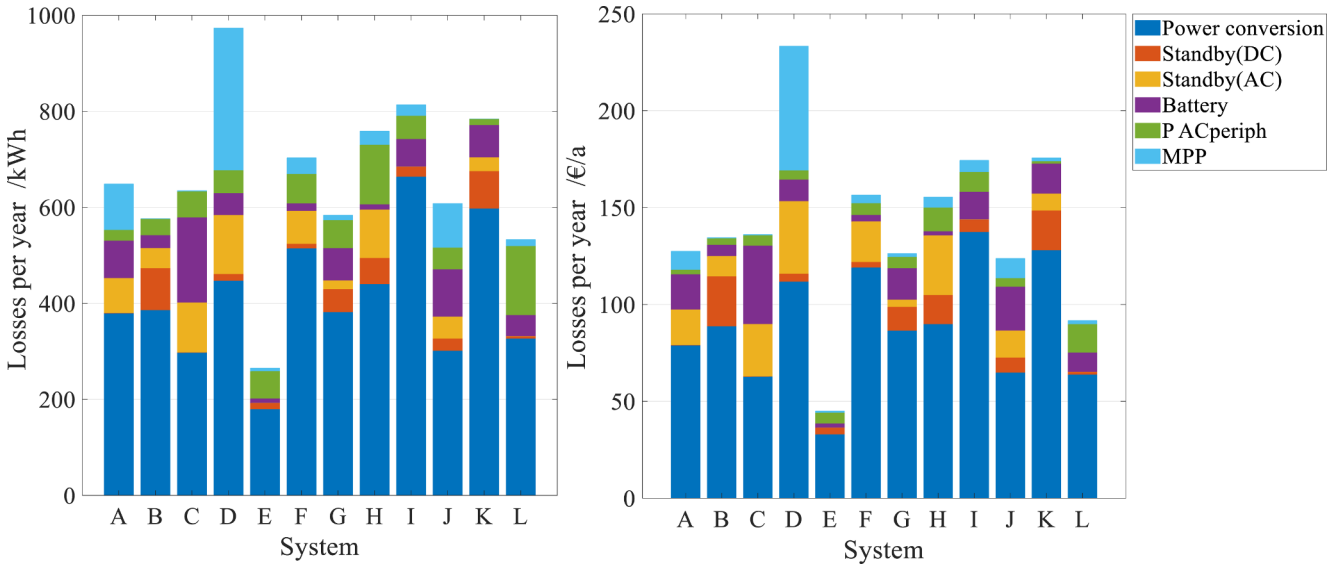

Fig. 17. Energy (left) and monetary (right) losses for a reference year using the VDI 4655 profiles.

resulting monetary losses in all systems are due to conversion losses. While some systems show high losses due to a lower battery efficiency or standby consumption, they are almost non-existent in other systems. This suggests that losses due to battery efficiency and standby consumption can be greatly reduced by further developments. This has already been confirmed for newer devices. In addition, only a few systems show MPP tracking losses. These mostly occur in DC-coupled systems from manufacturers who are not long-term experienced in the PV inverter industry. Therefore MPP tracking losses are another a good example for losses which can be further reduced in the future.

Systems with high conversion losses usually also have very high total losses and thus low system efficiencies. System I is a good example, even if the battery and standby losses are quite low, the system performs poorly in the overall comparison. System C is an exception to the above-mentioned rule – although it has a very high power conversion efficiency it still ends up with average to high losses and a rather low system efficiency which in this case is due to the unusually low battery efficiency (see Fig. 5).

4. Discussion

4.1. Comparison of the results with other factors affecting performance of PV home storage systems

In addition to the above-mentioned factors, the quality of the control algorithm and the control strategy also affect the system performance. Investigations have already been carried out and published on the storage systems currently under investigation. The results listed in the following serve to facilitate the interpretation of the results presented in this paper.

The control quality of the systems under test vary widely, specifically due to different durations of dead time and settling time in the control loop. A slow control algorithm with long dead times and/or settling times leads to an unnecessary exchange of energy with the grid. The measurements of the 12 systems under test show dead times of between <0.2 and 19.8 s and settling times of between 0.8 and 63.5 s. Monetary losses due to a slow control algorithm were reported to be up to €40 per annum [25,32], which is in the middle range of standby losses, in the upper range of battery efficiency losses and in the lower range of conversion losses.

Another aspect to consider is the effect of the control strategy on battery aging. In the case of lithium-ion batteries as with most cell chemistries, aging is accelerated if the battery spends too much time at high SOC levels [33]. This can to a large extent be avoided by employing an intelligent control strategy that includes forecasts of load and generation. Munzke et al. [6] describe a methodology to determine the economic effects of different charging strategies. Using the methodology described as well as the values given and applying the electricity costs of 30.46 cents and a feed-in tariff of 9.87 cents given in this article, losses of €41 to €295 [3] can be calculated over the lifetime of the systems. With the indicated lifetime of 7.6 and 14.6 years [6], the losses over the lifetime correspond to losses of between €3.7 and €22 per annum. How high the monetary effects are obviously depends on the charging strategy of the systems as well as the sensitivity of the batteries towards a higher degradation at high SOC levels. Another benefit of controlled and intelligent charging is that the battery is not fully charged too early in the day, so that the excess power at midday can still be stored and does not have to be fed into the grid or even throttled. Munzke et al. [6] calculate losses of 61.7 kWh and 104.2 kWh per annum due to an excess power limitation of the household to 70 % of the installed PV peak power. Using the current electricity price and the current feed-in tariff, these losses result in monetary losses of €5.8 to €10.3 per annum.

Thus, monetary losses due to a bad control quality can be up to €40 per year. Monetary losses due to a non-intelligent charging strategy can range between €3.7 and €22 per year due to increased battery aging and between €5.8 and €10.3 due to possible PV power throttling. Compared to these losses, however, the losses shown in this paper (see Table 6) can be in the same range, but are also significantly higher for most systems. Efficiency losses therefore represent the largest part of the losses and thus have the greatest influence on the performance of the PV home storage system.

Table 6
Annual energy and monetary losses.

	Loss kWh/a	Loss €/a
Standby consumption	2 to 55	1 to 46
Battery efficiency	9 to 77	2 to 40
Power electronics efficiency	180 to 664	33 to 137
MPPT	~1 to 296	1 to 81
Losses of peripheric components	13 to 144	1 to 15

5. Conclusion and outlook

The paper presents a methodology to compare the efficiency of storage systems under real operating conditions. For this purpose, so-called reference days are used. The PV home storage systems are all operated under the same conditions in the laboratory and are compared on the basis of their system and battery efficiency as well as on the basis of the occurring losses due to the battery losses, power conversion losses and standby consumption. The reference day measurements allow one to determine the possible monetary losses (in €/a) caused by each of the various factors. A method to calculate the losses is presented in this paper. The results of 12 storage systems are presented and analysed in detail to determine which losses have the greatest influence on the system efficiency and the economic viability of PV home storage systems.

The system efficiency of the systems under test ranges between 81.9 % and 94.1 %. It is mainly influenced by losses due to conversion losses, battery losses, standby consumption and losses of peripheric components. The battery efficiency of the investigated systems is between 78.4 % and 99.0 %. This leads to the annual losses listed in Table 6. How high the losses are depends mainly on the efficiency of the battery and not on its capacity. The largest energy and conversion losses in all systems are due to conversion losses (see Table 6). The losses of the PV2AC and PV2BAT&AC paths make up the largest porportion of energy losses in most of the systems studies. However, their share of monetary losses is significantly lower for most of the systems. Although the charging losses are only slightly lower than the discharging losses in terms of energy losses, they are significantly lower in terms of monetary losses. This is mainly due to the fact that losses of the conversion paths PV2AC, AC2BAT and PV2BAT&AC often only lead to a reduction in grid feed-in (9.87 cent/kWh), whereas losses during discharging (BAT2AC and PV&BAT2AC) mostly lead to an increase in grid consumption (30.46 cent/kWh).

In addition it has been shown that the systems have largely differing efficiencies, especially under partial load. This has the largest impact for battery discharging, since a large proportion of the discharge power lies below 1 kW in household applications (for some systems up to 100 %). Analysis of several different load profiles has confirmed that the same applies to other load profiles. For this purpose 9 ADRES HH were examined. Between 73.7 % and 75.4 % (66.2 % and 68.3 %) of the households' consumption occurs at a power smaller than 1.5 kW (1 kW). As a consequence, it is advantageous for storage systems in household applications to be optimised in terms of their efficiency at partial load for the pathway BAT2AC (battery discharge). Here, for example, SiC-based MOSFET converters could bring improvements [34].

While some systems show high losses due to a lower battery efficiency, standby consumption, losses of peripheric components as well as MPP-tracking losses, they are nearly non-existent in other systems. This leads to the conclusion that these losses can be reduced by further development.

The individual losses can be summed up to give a total loss which lies between €44 and €174 per annum excluding MPP-tracking losses and between €44 and €238 per annum including MPP-tracking losses.

The analysed losses in this paper have a higher influence on monetary losses and therefore on the economic viability of PV home storage systems than losses due to a bad control quality or a non-intelligent charging strategy. However, how the charging strategy affects the efficiency of the system during charging and discharging has not yet been investigated. It may be part of further work.

In order to be able to make a statement about the actual value of storage systems, further investigations between efficiency and the resulting losses and actual investment costs and profits have to be carried out. This is however beyond the presented work and is a part of further investigations.

Declaration of Competing Interest

The authors declare that they have no known competing financial interests orpersonal relationships that could have appeared to influence the work reported in this paper.

Acknowledgements

This work contributes to the research performed at (KIT-BATEC) KIT Battery Technology Center and CELEST (Center for Electrochemical Energy Storage Ulm-Karlsruhe). The results presented here were generated within the "Safety First" project (funding code: 03ET6055A), funded by the Federal Ministry for Economic Affairs and Energy (BMWi). The authors thank the project management organisation Jülich (PtJ) and the BMWi. The load profile data in second resolution were recorded within the "ADRES-CONCEPT" research project (EZ-IF: Concept development for ADRES – Autonomous Decentralised Regenerative Energy Systems, Project Nr.: 815 674) [29]. This project was funded out of the Climate and Energy funds and was carried out within the programme "ENERGIE DER ZUKUNFT". The authorts thank Anna Sina Starosta for her support regarding spelling and grammar.

References

[1] J. Figgener, P. Stenzel, K.-P. Kairies, J. Linßen, D. Haberschusz, O. Wessels, G. Angenendt, M. Robinius, D. Stolten, D.U. Sauer, The development of stationary battery storage systems in Germany – A market review, J, Energy Storage 29 (2020) 101153https://doi.org/10.1016/j.est.2019.101153.
[2] N. Lebedeva, D. Tarvydas, I. Tsiropoulos, European Commission, Joint Research Centre, Li-ion batteries for mobility and stationary storage applications: scenarios for costs and market growth., 2018. http://publications.europa.eu/publication/manifestation_identifier/PUB_KJNA29440ENN (accessed June 20, 2020).
[3] N. Munzke, Dimensionierung und Auslegung von Photovoltaik-Speichersystemen, Stromspeicher Für Gewerbe Ind. Tech. Auswahl Auslegung Mit Anm. Für Heimspeicher, 1st ed., Berlin Wien Zürich, Beuth, 2018, pp. 114–153.
[4] G. Angenendt, S. Zurmühlen, H. Axelsen, D.U. Sauer, Comparison of different operation strategies for PV battery home storage systems including forecast-based operation strategies, Appl. Energy. 229 (2018) 884–899 https://doi.org/10.1016/j.apenergy.2018.08.058.
[5] J. Li, M.A. Danzer, Optimal charge control strategies for stationary photovoltaic battery systems, J. Power Sources 258 (2014) 365–373 https://doi.org/10.1016/j.jpowsour.2014.02.066.
[6] N. Munzke, B. Schwarz, M. Hiller, Intelligent control of household Li-ion battery storage systems, Energy Procedia 155 (2018) 17–31 https://doi.org/10.1016/j.egypro.2018.11.069.
[7] G. Angenendt, S. Zurmühlen, R. Mir-Montazeri, D. Magnor, D.U. Sauer, Enhancing Battery Lifetime in PV Battery Home Storage System Using Forecast Based Operating Strategies, Energy Procedia 99 (2016) 80–88 https://doi.org/10.1016/j.egypro.2016.10.100.
[8] N. Munzke, B. Schwarz, F. Büchle, J. Barry, Lithium-Ionen Heimspeichersysteme, Performance auf dem Prüfstand, 2017 Kloster Banz Bad Staffelstein.
[9] T. Tjaden, J. Weniger, C. Messner, M. Knoop, M. Littwin, K.-P. Kairies, D. Haberschusz, H. Loges, V. Quaschning, Offenes Simulationsmodell für netzgekoppelte PV-Batteriesysteme, in: Kloster Banz, Bad Staffelstein (2017).
[10] A. Benatiallah, R. Mostefaou, K. Bradja, Performance of photovoltaic solar system in Algeria, Desalination 209 (2007) 39–42 https://doi.org/10.1016/j.desal.2007.04.006.
[11] T. Ma, H. Yang, L. Lu, Performance evaluation of a stand-alone photovoltaic system on an isolated island in Hong Kong, Appl. Energy. 112 (2013) 663–672 https://doi.org/10.1016/j.apenergy.2012.12.004.
[12] M. Braun, K. Büdenbender, D.U. Sauer, D. Magnor, A.U. Schmiegel, Charakterisierung von netzgekoppelten PV-Batterie-Systemen - Verfahren zur vereinfachten Bestimmung der Performance, 25 Symp. Photovoltaische Solarenergie 2010, 2010, pp. 462–467.
[13] BVES, BSW, Effizienzleitfaden für PV-Speichersysteme, (2017).
[14] Efficiency guideline for PV storage systems V 2.0, (2019).
[15] C. Messner, J. Kathan, C. Seitl, S. Hofmüller, R. Bründlinger, Efficiency and Effectiveness of PV Battery Energy Storage Systems for Residential Applications - Experience from Laboratory Tests of Commercial Products, in: München, 2016. https://doi.org/10.4229/EUPVSEC20162016-6CO.12.1.
[16] K.-P. Karais, D. Haberschusz, J. van Ouwerkerk, J. Strebel, O. Wessels, D. Magor, J. Badeda, D.U. Sauer, Wissenschaftliches Mess- und Evaluierungsprogramm Solarstromspeicher Jahresbericht 2016, Institut für Stromrichtertechnik und Elektrische Antriebe der RWTH Aachen, 2016.
[17] J. Figgener, D. Haberschusz, K.-P. Karies, O. Wessels, B. Tepe, M. Ebbert, R. Herzog, D.U. Sauer, Wissenschaftliches Mess- und Evaluierungsprogramm Solarstromspeicher 2.0 Solarstromspeicher Jahresbericht 2017, Institut für Stromrichtertechnik und Elektrische Antriebe der RWTH Aachen, 2017.

[18] S. Maier, J. Weniger, N. Böhme, V. Quaschning, Simulationsbasierte Effizienzanalyse von PV-Speichersystemen, in: 34 PV-Symp. 19 Bis 21 MÄRZ 2019 Klost. Banz Bad Staff., Bad Staffelstein, n.d.: pp. 209–219.
[19] J. Weniger, T. Tjaden, V. Quaschning, Vergleich verschiedener Kennzahlen zur Bewertung der energetischen Performance von PV-Batteriesystemen, in: Kloster Banz, Bad Staffelstein, 2017.
[20] J. Weniger, S. Maier, L. Kranz, N. Orth, N. Böhme, V. Quaschning, Stromspeicher-Inspektion2018, Version 1.1, (2018).
[21] J. Weniger, N. Orth, N. Böhme, V. Quaschning, Stromspeicher-Inspektion 2019, Version 1.0, (2019).
[22] J. Weniger, S. Maier, N. Orth, V. Quaschning, Stromspeicher-Inspektion 2020, Version 1.0, (2020).
[23] F. Niedermeyer, J. von Appen, T. Kneiske, M. Braun, A. Schmiegel, N. Kreutzer, M. Rothert, A. Frohner, Innovative Performancetests für PV-Speichersysteme zur Erhöhung der Autarkie und des Eigenverbrauchs, Photovoltaische Solarenergie, Kloster Banz Bad Staffelstein (2015) 178–179.
[24] N. Orth, J. Weniger, T. Tjaden, N. Munzke, B. Schwarz, F. Büchle, C. Messner, J. Figgener, D. Haberschusz, V. Quaschning, Vergleich der Energieeffizienz verschiedener PV-Speichersystemkonzepte, Bad Staffelstein, Kloster Banz, 2018.
[25] N. Munzke, J. Barry, B. Schwarz, Performance Evaluation of Household Li-Ion Battery Storage Systems, in: München, 2016. https://doi.org/10.4229/EUPVSEC20162016-5AO.9.5.
[26] B. Boeckl, T. Kienberger, Sizing of PV storage systems for different household types, J. Energy Storage 24 (2019) 100763 https://doi.org/10.1016/j.est.2019.100763.
[27] J. Weniger, T. Tjaden, V. Quaschning, Sizing of Residential PV Battery Systems, Energy Procedia 46 (2014) 78–87 https://doi.org/10.1016/j.egypro.2014.01.160.
[28] VDI, VDI-Richtlinie: VDI 4655 Referenzlastprofile von Ein- und Mehrfamilienhäusern für den Einsatz von KWK-Anlagen, (2008).
[29] A. Einfalt, A. Schuster, C. Leitinger, D. Tiefgraber, M. Litzlbauer, S. Ghaemi, D. Wertz, A. Frohner, C. Karner, EA: ADRES-Concept – Konzeptentwicklung für ADRES - Autonome Dezentrale Regenerative Energie Systeme, Wien, 2012, http://www.ea.tuwien.ac.at/projects/adres_concept/EN/ accessed June 24, 2016.
[30] Bundesnetzagentur, Bundeskartellamt, Monitoringbericht 2019, 2020. https://www.bundesnetzagentur.de/SharedDocs/Mediathek/Berichte/2019/Monitoringbericht_Energie2019.pdf?_blob=publicationFile&v=5 (accessed January 22, 2020).
[31] Fraunhofer ISE, Aktuelle Fakten zur Photovoltaik in Deutschland, (2020). www.pv-fakten.de.
[32] J. Weniger, T. Tjaden, J. Bergner, V. Quaschning, Auswirkungen von Regelträgheiten auf die Energieflüsse in Wohngebäuden mit netzgekoppelten PV-Batteriesystemen, in: Kloster Banz, Bad Staffelstein (2016).
[33] P. Keil, S.F. Schuster, J. Wilhelm, J. Travi, A. Hauser, R.C. Karl, A. Jossen, Calendar Aging of Lithium-Ion Batteries I. Impact of the Graphite Anode on Capacity Fade, J. Electrochem. Soc. 163 (2016) A1872–A1880 https://doi.org/10.1149/2.0411609jes.
[34] L. Probst, D. von Kutzleben, C. Armbruster, C. Schöner, Partial-Load Optimization of a High-Voltage Residential Battery Converter with Silicon Carbide MOSFETs, PCIM Eur. 2019 Int. Exhib. Conf. Power Electron. Intell. Motion Renew, Berlin, Energy Energy Manag. CD-ROM, VDE-Verlag, 2019, p. 7.